IN-14

154181

p. 52

NASA Contractor Report 185709

Advanced Underwater Lift Device

David T. Flanagan
Robert C. Hopkins

March 1993

NASA

דר

NASA Contractor Report 185709

Advanced Underwater Lift Device

David T. Flanagan
Krug Life Sciences
Houston, TX 77058

Robert C. Hopkins
University of Houston, Clear Lake
Houston, TX 77058

NASA

National Aeronautics
and Space Administration

Scientific and Technical
Information Branch

Contents

Tables

Figures

Appendices

ABSTRACT

Title: Advanced Underwater Lift Device

Authors: David T. Flanagan, B.S.
Robert C. Hopkins, Ph.D.

Flexible underwater lift devices ("lift bags") are used in underwater operations to provide buoyancy to submerged objects. Commercially available designs are heavy, bulky, and awkward to handle, and thus are limited in size and useful lifting capacity. An underwater lift device having less than 20% of the bulk and less than 10% of the weight of a commercially available models has been developed. The design features a dual membrane envelope, a nearly homogeneous envelope membrane stress distribution, and a minimum surface-to-volume ratio. A proof-of-concept model of 50 kg capacity was built and tested. Originally designed to provide buoyancy to mock-ups submerged in NASA's weightlessness simulators, the device may have application to water-landed spacecraft which must deploy flotation upon impact, and where launch weight and volume penalties are significant. The device may also be useful for the automated recovery of ocean floor probes or in marine salvage applications.

Key Words: Marine technology, underwater structures, lift devices, spacecraft recovery, flotation

INTRODUCTION

Flexible underwater lift devices ("lift bags") are used by divers during underwater salvage and construction operations to provide buoyancy to submerged objects. An underwater lift bag consists of a flexible impermeable envelope, and a harness that connects the envelope to the load. The harness is first connected to the submerged object, then air is introduced into the envelope. The buoyancy provided by the air trapped in the envelope is transmitted to the load by the harness.

A significant advantage of lift bags is their portability. They are flexible and may be folded for transport. However, currently available lift bags, particularly those of large lifting capacity, are heavy, bulky, and awkward to handle. Generally, larger commercial lift bags cannot be carried underwater until actually needed because of their excessive bulk and weight. This adversely affects underwater operations. For example, a search and salvage mission requires a minimum of two sorties. The object to be recovered is located and marked during the first sortie. A second sortie is then needed to obtain and deploy the lift bag and recover the object. Multiple underwater sorties reduce efficiency and complicate diving operations, particularly those carried out at significant depths.

Clearly, a lift bag of reduced bulk and weight would be useful in underwater operations.

OBJECTIVE

The objective of this project was to improve the design the underwater lift bag. Specifically, the study focused on enhancing portability and ease of use by reducing weight and bulk. A further objective was to produce a proof-of-concept model capable of lifting 50 kilograms in fresh water.

PROPOSED CONCEPTS

Three factors contribute to the weight and bulk of currently available lift bags. First, the material selected for the envelope is usually a stiff, heavy polymer-coated fabric. Second, the envelope shapes do not minimize the envelope surface-to-volume ratios. Third, these shapes do not allow the envelope membranes to distribute stress uniformly, which implies that some areas are needlessly strong, and therefore needlessly bulky. The following concepts are therefore proposed.

Membrane Material Redesign

The membrane of a lift bag envelope must fulfill two functions. It must provide mechanical strength and be impermeable to the trapped gas that provides the buoyancy. Current designs fulfill both functions with a single layer of material, usually canvas or nylon

2

coated with a polymer. The fabric provides the strength and the polymer coating provides the impermeability. This type of material, often found in inflatable rafts and life vests, is both heavy and bulky.

The requirements for strength and impermeability can be separated, and a dual membrane approach adopted. The outer membrane can be a porous fabric selected for mechanical strength. The inner membrane can be a thin polymer selected for impermeability. The inner membrane would be larger than the outer membrane, would conform to it, and would not be bonded to it except at the opening of the device. Since neither material must fulfill the requirements for both strength and impermeability, the pool of candidate materials for each membrane would be significantly greater.

In a previous unpublished study, underwater lift devices with dual membrane envelopes shaped like cylinders and rectangular sleeves were successfully deployed. Although localized areas of high stress were noted on the envelope membranes, the dual membrane concept seemed feasible (1).

The dual membrane approach is also used for gas containment in the design of the Pressure Garment Assembly of the Shuttle Extravehicular Mobility Unit (spacesuit). A gas permeable outer layer provides structural strength while a lighter, thinner, inner layer provides impermeability (2).

Envelope Geometry Optimization

Many shapes are available for underwater lift device envelopes. An envelope geometry with a minimum surface-to-volume ratio will minimize the amount of material required per unit lifting capacity, and thus reduce the bulk and weight of the lift bag. A homogeneous stress distribution in the membrane of the envelope is also desirable. A nonhomogeneous stress distribution implies that some areas are needlessly strong, and therefore unnecessarily heavy and bulky.

The envelope shape, then, must provide a minimum surface-to-volume ratio and a homogenous stress distribution. These criteria can be fulfilled by modelling the envelope after a **pendant drop**. A pendant drop is the equilibrium shape of a liquid droplet, in which the gravitational force acts to draw the liquid away from a substrate to which it is attached. A drop of water hanging from the tip of an eye dropper is an example. The surface tension of the fluid insures that the pendant drop exhibits the lowest possible surface-to-volume ratio for its physical environment. An underwater lift device modelled after a pendant drop would therefore also exhibit a minimum surface-to-volume ratio. Also, the surface tension of a pendant drop is everywhere constant. Since the surface tension can be equated to the membrane stress of an underwater lift device modelled after a pendant drop, a homogenous membrane stress distribution can be assured. Because of these factors, the pendant drop can serve as a model for an underwater lift device.

3

APPROACH

Material Selection

Significant reductions in lift bag bulk and weight can be achieved by adopting a dual membrane envelope. The best material for each of the two membranes must be selected based on a comprehensive trade study of available materials.

Parameters for any trade study of materials for the outer membrane and harness material of an underwater lift device will include, at a minimum, mechanical strength, dimensional stability, weight, workability, abrasion resistance, ultraviolet light resistance, salt water resistance, availability, and cost.

Material Testing

A lift device modeled on the pendant drop will have a specific shape. It will experience stress and exhibit strain under load. Failure to correct for stress can result in deformation of the device from optimum shape and induce a nonhomogeneous stress distribution. Correction for stress requires knowledge of a material's tensile modulus. Consequently, these values must be determined for both membrane and harness materials through testing.

Also, the outer membrane of the envelope is made of fabric pieces that must be joined together. One method of joining is sewing, which can cause dimensional changes in fabric structures. Sewing a seam can shorten its linear dimension by as much as ten percent, depending on fabric type, stitch selected, number of stitches per inch, thread tension, operator technique, and other factors (3). The extent of this sewing "take-up" must be determined.

Tensile Modulus Testing

The tensile modulus relates stress to strain

$$strain = \frac{1}{Y} \; stress$$

or

$$\frac{\Delta L}{L} = \frac{1}{Y} \frac{F}{A}$$

where Y is Young's Modulus with units in newtons per meter squared (N/m^2), $\Delta L/L$ is the strain, or change in length per unit original length, and F/A is the stress applied in N/m^2. Although this equation can be directly applied to fabric or cord, it is convenient to modify the equation to reflect the symmetry of the tested item. For the outer membrane material of constant thickness, the equation for tensile modulus becomes

$$\frac{\Delta L}{L} = \frac{1}{Y_m} \frac{F}{w}$$

where Y_m is the modulus in N/m and w is the width of the strip under test in meters. The harness material equation is similar, but because the cross-sectional area can be treated as approximately constant, the area parameter can be eliminated:

$$\frac{\Delta L}{L} = \frac{1}{Y_h} F$$

In this equation the modulus Y_h is rendered simply in newtons.

Sewing Take-up Testing

The sewing take-up of the seams can be determined using coupons of fabric. The length of a doubled piece of outer membrane fabric can be measured before and after sewing, and the decrease in length noted.

Envelope Geometry Optimization

Background Study

The shape of a pendant drop varies with respect to several parameters, including volume, the densities of the contained and surrounding fluids, the interfacial surface tension, and the strength of the gravitational field. Pendant drops are reviewed by Hartland and Hartley in "Axisymmetric Fluid-Liquid Interfaces" (4).

Notation for the pendant drop is shown in Figure 1. In the nomenclature of reference 4, significant variables include:

   b: the radius of curvature at the apex. Note that $b=r_1=r_2$ at the apex
   r_1: the radius of curvature in the meridional plane of the surface at any point
   r_2: the radius of curvature orthogonal to r_1. The origin of r_2 is always on the axis of symmetry. Over any incremental area dA on the surface, r_2 is perpendicular to r_1
   z: the vertical distance along the axis from the apex. Note z = 0 at the apex
   x: the radius of the drop in the plane perpendicular to the axis of symmetry at any point z on the axis of symmetry
   s: the distance on the surface of the drop from the apex to the plane of the circle defined by the radius x
   θ: angle of the line tangent to the surface at position s with respect to a plane tangent to the apex (labelled "ANGLE" in Table I)
   a: the area of the surface of the drop from the apex to the plane of the circle defined by the radius x
   v: the volume of the drop from the apex to the plane of the circle defined by the radius x

5

The dimensionless parameter B is the radius of curvature at the apex of a pendant drop. It implicitly defines the overall shape of the pendant drop. Figure 2, taken from reference 4, shows the profiles of several pendant drops with respect to log(B). It is convenient to refer to log(B) as the "shape factor."

The profile of a particular pendant drop must be determined by numerically solving a second-order ordinary differential equation. Hartland and Hartley used a fourth-order Runge-Kutta algorithm coded in Fortran IV for this purpose. They provide data tables for 83 selected values of log(B) from -2 to +1. The data table for the pendant drop for which log(B) = -0.24 is presented in Table I. Accuracy better than one part in 10^6 is claimed.

An important feature of Hartland and Hartley's work is that the values given in each table are nondimensionalized by a factor c, where c is the product of the density difference between the contained fluid and the surrounding medium and the acceleration field divided by the surface tension

$$c = \frac{\Delta \rho g}{\sigma} \qquad [units = m^{-2}]$$

This parameter includes all of the essential characteristics of a pendant drop and its physical environment. To recover actual data, each linear value provided in the tables must be divided by $c^{1/2}$. Correspondingly, area values must be divided by c, and volumes by $c^{3/2}$. For example, the radius of curvature at the apex in meters would be $b=B/c^{1/2}$.

Shape Selection

The pendant drop shape best suited for application to underwater lift devices must be determined. The important parameters are:

Plane of Truncation: A plane of truncation is perpendicular to the axis of symmetry and divides a pendant drop into two sections. The section containing the apex is pertinent to the design of an underwater lift device. The plane of truncation is identified by the value of θ at the point on the surface of the pendant drop where the plane of truncation intersects it.

Selection of the plane of truncation directly affects harness design. The harness is attached to the opening of the envelope at the plane of truncation. Each harness leg must lie in the plane tangent to the envelope surface at its attachment point (Figure 3).

Surface-to-Volume Ratio: The surface-to-volume ratio directly affects the bulk and weight of an underwater lift device. Minimizing this parameter will minimize both bulk and weight.

Membrane Stress: Minimizing membrane stress will allow the use of lighter, less bulky materials to be used in the design of the outer membrane.

Modelling Approach

Gore Design

The smoothly curved surface of a pendant drop cannot be exactly duplicated using flat pieces of fabric, but it can be approximated. Dividing the surface into a finite number of gores (as in a parachute) seems an obvious approach, but the best method of forming such gores needs to be determined. Three candidate methods of developing the needed gore patterns are referred to as the **x-radius method**, the **r_2-perp method**, and the **r_2-radius method**.

X-Radius Method

The data table for a pendant drop of a particular value of log(B) provides dimensionless data with respect to selected values of θ (labelled "ANGLE" in Table I). If s represents a distance from the apex along a gore axis, the width of the gore w at that point s can be approximated by

$$w = \frac{2\pi x}{n}$$

where n is the number of gores selected (Figure 4).

The radius x is only perpendicular to the surface of a pendant drop when θ = 90 degrees. Thus, perpendiculars constructed from the gore axis based on the above width would not accurately define the gore borders. As an approximate alternative, arcs of the appropriate radius ($\frac{1}{2}$w) can be struck from each point s on an arbitrary gore axis. Line segments tangent to the arcs may then be drawn to define the gore edges.

R$_2$-Perp Method

The r_2-perp method requires erecting perpendiculars to the axis of the gore at each known point s along that axis. The length of each perpendicular can be calculated as follows.

Referring to Figure 4, for the selected number of gores n, the central angle in the plane of the circle defined by the two radii x that intersect the gore borders is

$$\Delta = \frac{2\pi}{n}$$

The secant line sl can be drawn and is found by

$$sl = 2x\sin\frac{\pi}{n}$$

Then, the value for r_2 is calculated from x and θ associated with the point s

7

$$r_2 = \frac{x}{\sin\theta}$$

And, using r_2 and the secant line sl, the angle α in the plane of r_2 and sl is determined by

$$\frac{sl}{2r_2} = \sin\left(\frac{\alpha}{2}\right)$$

or

$$\alpha = 2\arcsin\left(\frac{sl}{2r_2}\right)$$

Substituting the values previously obtained for r_2 and sl

$$\alpha = 2\arcsin\left(\frac{2x\sin\frac{\pi}{n}}{\frac{2x}{\sin\theta}}\right)$$

and simplifying

$$\alpha = 2\arcsin\left(\sin\frac{\pi}{n}\sin\theta\right)$$

Now, if r_2 can be assumed to be the radius of a circle over an incremental $d\alpha$ in the plane defined by itself and the secant line, the gore width w on the surface is related to the circumference of that circle by

$$\frac{w}{2\pi r_2} = \frac{\alpha}{2\pi}$$

or

$$w = \alpha\, r_2$$

Substituting the values previously obtained for α and r_2 gives

$$w = \frac{2x\arcsin\left(\sin\frac{\pi}{n}\sin\theta\right)}{\sin\theta}$$

This value, divided in half ($\frac{1}{2}w$), is the length of the perpendicular to the gore axis to be erected at each point s. Once the perpendiculars are in place, their endpoints can be joined by line segments to define the gore edges.

R₂-Radius Method

The r_2-radius method is similar to the r_2-perp method, except that instead of erecting perpendiculars, arcs are struck whose radii are

8

calculated in the same manner that the lengths of the perpendiculars are found in the r_2-perp method. With the arcs in place, tangent lines can be drawn as in the x-radius method to define the gore edges.

The overall differences between the x-radius and r_2-radius methods are small. Figure 5 compares the differences in the radii of the arcs used to fabricate the gores of a hypothetical underwater lift device of 100 kilogram capacity.

As the number of gores n approaches infinity, the shape will approach the ideal theoretical shape regardless of the modelling method used.

Correction For Stress

The dimensional data for gore construction and harness leg length need to be corrected for the stress on the basis of the tensile moduli of the materials. This can be done by multiplying each linear dimension by an experimentally determined correction coefficient. The stress correction coefficient for the outer membrane material can be found as follows:

As previously discussed, the equation for the tensile modulus of the membrane material can be written

$$\frac{\Delta L}{L} = \frac{1}{Y_m} \frac{F}{w}$$

The left-hand side of this equation is the ratio of the change in length ΔL due to stress to the initial unstressed length L. The right-hand side contains a term for stress in force per unit width. This stress F/w is the uniform envelope membrane stress, which is equivalent to the surface tension of a pendant drop σ, or

$$\frac{F}{w} = \sigma$$

so the equation for tensile modulus becomes

$$\frac{\Delta L}{L} = \frac{1}{Y_m} \sigma$$

Adding unity to both sides

$$\frac{L}{L} + \frac{\Delta L}{L} = \frac{1}{Y_m} \sigma + \frac{Y_m}{Y_m}$$

or

$$\frac{L + \Delta L}{L} = \frac{\sigma + Y_m}{Y_m}$$

Now let L_s be the desired final, stressed, dimension. It is the combination of the initial unstressed length L and the change in length due to stress, ΔL:

$$L_s = L + \Delta L$$

Therefore

$$\frac{L_s}{L} = \frac{\sigma + Y_m}{Y_m}$$

or

$$L = L_s \frac{Y_m}{\sigma + Y_m}$$

This equation states that a **corrected** unstressed dimension L is equal to the desired, final, stressed length L_s times the correction factor F_c, where

$$F_c = \frac{Y_m}{\sigma + Y_m}$$

Thus, as the membrane stress σ increases, the stress correction coefficient decreases, which in turn reduces the linear dimensions to which it is applied.

A stress correction coefficient for the harness material can be obtained in an analogous fashion.

Correction For Sewing Take-Up

A sewing take-up correction coefficient is needed to compensate for reduction in seam length which may occur during fabrication. Take-up may be calculated by

$$T_f = \frac{L_f}{L_o}$$

where L_o would be the original length of the test coupon, L_f the final length of the coupon after sewing, and 100% x T_f the percent of the original length of the coupon that remained after sewing. The correction factor applied to the linear dimensions would then be $1/T_f$.

10

Correction for Modelling Method

The modelling methods above approximate a curved surface using planar segments. This approach can induce departures from the optimum theoretical shape. Point loading or other surface discontinuities at the envelope/harness interface may also have such an effect. Therefore the actual volume of the envelope may vary from the theoretical volume. To compensate for this, a correction factor can be defined. If V_a is the actual volume of a model as determined by experiment and V_t is its theoretical volume, then

$$V_f = \frac{V_a}{V_t}$$

where 100% x V_f would be the percent change of the actual volume with respect to the theoretical volume. The correction factor to be applied to an initial, desired volume would then be $1/V_f$.

Computer Design Program

A computer is ideally suited for modelling the pendant drop shape and for developing the gore planform and other construction data. The dimensionless data for the selected pendant drop shape can be incorporated into a computer program. Correction factors for materials elasticity, sewing take-up, and modelling method can also be included. The program would be interactive, allowing input to be modified and output to be displayed on the screen. Ideally, input would consist solely of the desired capacity of the lift device. As a minimum, output would consist of the theoretical parameters of the stressed lift device, and the corrected data required to manufacture the envelope gore pattern and harness components of the device.

Model Testing

Suspended Testing

The actual capacity and shape of a model lift device while under load can be tested by suspending the lift bag by its harness confluence point and filling it with water. Because the volume of water a lift device would contain in this configuration is approximately equal to the amount of water it would displace in use underwater, the forces on all parts of the lift device would be nearly identical to those that would occur underwater if the lift bag were filled with air. This test method would provide a comfortable and logistically simple method of observing the models under load. A logical alternative would be to do all testing underwater but with much greater inconvenience.

Capacities can be obtained by filling models suspended by their harness confluence to maximum capacity, and then quantifying the contained water by weighing or by measuring volume.

To evaluate a model for proper shape, its actual profile can be compared to its theoretical profile in two ways. A less accurate method would involve visually comparing the profile of the suspended, water-filled lift device with a representation of its ideal shape, such as a correctly scaled silhouette. Such a silhouette can be readily fabricated from the data for each shape factor log(B) given in reference 4. Greater accuracy could be obtained using a simple photogrammetric technique. First, a silhouette of the theoretical shape can be photographed with slide film using a camera equipped with a telephoto lens. The long focal length of the lens would provide a relatively flat field, and the camera-to-subject distance could be adjusted so the image filled the frame. Then, without moving the camera, the silhouette could be replaced by the suspended, water-filled lift device, which would also be photographed. The two slides could then be projected from the same distance onto a screen and various comparative linear measurements taken.

Bulk and Mass Comparison Testing

An objective of this project is to reduce the bulk and weight of a lift bag. To quantify bulk and weight reduction, models produced during this project must be compared to commercially available lift bags of equal capacity. Weight can be obtained with reasonable accuracy using a laboratory balance. The volume of a packaged flexible device is considerably more difficult to determine accurately (5). However, estimates can be made by measuring linear dimensions of the folded lift devices.

Underwater Testing

Models also can be evaluated underwater. Test parameters of interest would be ease of transport, ease of inflation, general stability on ascent and at equilibrium on the surface with various suspended loads. Underwater photographs would be useful for later evaluations of shape and performance.

MATERIALS & METHODS

A summary of the models constructed in the course of this study may be found in Appendix A. Details of the materials and methods used to construct and test these models are presented in Appendix B.

RESULTS & DISCUSSION

Material Selection

Outer Membrane

The material selected for the outer membrane was a parachute canopy fabric manufactured to the specifications of MIL-C-7020G Type I (6). Type I fabric was developed in World War II as a replacement for oriental silk, and continues to be specified for military and emergency personnel parachutes today. It is fabricated in large

quantities to consistent quality specifications, is widely available, and is inexpensive. Its disadvantages include poor resistance to ultraviolet light and abrasion, and poor dimensional stability (3). Pertinent characteristics taken from the military specification are given in Table II.

Harness

Two types of cord used as suspension lines in various parachutes were selected as harness material for this study: MIL-C-5040G Type IA and Type IIA (7). Type IA was used for the smaller models, and Type IIA for the largest lift device. Both are lightweight hollow braided nylon cords. Pertinent characteristics taken from the military specification are given in Table III.

Inner Membrane

Off-the-shelf polyethylene trash bags were used as inner membranes. Various shapes and sizes were employed, depending on the size of the model being tested. The primary selection criterion was that the polyethylene bag be large enough to conform to the outer membrane without experiencing tensile stress.

Material Testing

Tensile Modulus Testing

The tensile moduli for both materials increase with the total amount of stress. A graph showing the modulus of the membrane material with respect to stress is shown in Figure 6. Figure 7 gives the same data for Type IIA harness material. Type IA harness material was not tested. The harness leg length of models equipped with Type IA harnesses was determined under load during suspended testing, thus knowledge of the tensile modulus of this material was not needed.

The relationship between stress and the tensile modulus is clearly not linear. Although both data sets seem qualitatively similar, an exponential curve provided the best fit for the membrane data, and a linear expression best described the harness material data. Why the same type of curve did not apply to both nylon materials is not completely understood, but may be related to the limited ranges tested. The membrane material was tested to 25% of its minimum rated ultimate tensile strength. The harness material was tested to only 17% of its minimum rated ultimate tensile strength. The harness material test data may therefore appear linear due to the more limited range tested.

The data may also have been influenced by the test procedure. Tensile modulus testing of such materials is difficult to perform accurately. The pseudo-plastic nature of the material, creep, variations in the orientation of the material in the clamps, undetected slippage, and, for nylon materials, variations in environmental conditions can affect the results.

13

Sewing Take-up Testing

The selected seam type shortened the linear dimension of a seam to about 98% of its original value. Thus $T_f = 0.98$ and $1/T_f = 1.02$.

Envelope Geometry Optimization

Shape Selection

Plane of Truncation: Possible values for the plane of truncation of the pendant drop were arbitrarily limited to $115 \leq \theta \leq 135$ degrees. Planes of truncation where $\theta < 115$ degrees would result in harness legs that were judged to be too long. Longer harness legs increase bulk. Conversely, planes of truncation where $\theta > 135$ degrees suggest excessively short harness legs. Since the load is greater on excessively short harness legs, they must be stronger and therefore made of bulkier material, again increasing bulk.

Limiting the range of θ to $115 \leq \theta \leq 135$ degrees limits the harness angle range to between 25 and 45 degrees (Figure 3).

Surface-to-Volume Ratio: The surface-to-volume ratios of a range of pendant drop shapes were evaluated where $115 \leq \theta \leq 135$ degrees. Considering the data available in reference 4, candidate pendant drop shapes include those for which $-2.0 \leq \log(B) \leq -0.24$. Pendant drops where $\log(B) > -0.24$ do not have values of θ falling within the chosen range of $115 \leq \theta \leq 135$ degrees. Of the candidate shapes, the pendant drop $\log(B) = -0.24$ exhibited a dimensionless surface-to-volume ratio of 4.179 where $\theta = 115$ degrees. The surface-to-volume ratios of other candidate shapes, within the applicable range of θ, were all greater than 4.179. This search is summarized in Figure 8.

Membrane Stress: The parameter c has been discussed previously:

$$c = \frac{\Delta \rho g}{\sigma}$$

Since the dimensionless value for volume V is related to actual volume v by

$$c^{\frac{3}{2}} = \frac{V}{v}$$

then

$$\sigma = \frac{\Delta \rho g}{v^{\frac{2}{3}}} V^{\frac{2}{3}}$$

Thus, membrane stress σ increases as the dimensionless volume V decreases for a fixed actual volume v.

The shape described by log(B) = -0.24 exhibits a dimensionless volume V = 1.053 at θ = 115 degrees. Shapes where log(B) ≤ -0.24 all have a lower value of V at θ = 115 degrees, and would therefore, if all other conditions remain constant, exhibit greater membrane stress for a given volume v.

Therefore, based on the above, the most suitably shaped pendant drop for modelling an underwater lift device has the shape factor log(B) = -0.24 and is truncated at θ = 115 degrees.

Computer Design Program

The interactive design program was written in generic BASIC on a personal computer and evolved with the project. For example, before tensile modulus and sewing take-up testing was performed, the program requested that arbitrary values be supplied for these parameters. Later, these values were supplied automatically by the program based on the programmed test data. Also, the program was modified as required to incorporate the gore modelling technique being investigated. Thirteen significant revisions were made to the original code. The most recent edition is listed in Appendix C.

Model Testing

Suspended Testing

Visual Profile Evaluation

X-Radius Method: The first three models were designed using the X-radius method. During visual examination a slight tendency towards flatness in the apex area was noted. Distortion of the envelope around the mouth of the model at the harness interface was also apparent.

The flatness in the apex area was probably due to the gore modelling method. As noted, the x-radius method accurately reflects the surface arc length only at a θ = 90 degrees. At all other values of θ, the surface arc length given by this method is greater than actual (Figure 4). Therefore, this method may produce "excess" gore material, especially at the apex, which would confer an oblate shape.

The envelope around the opening was distorted. Point loading of the periphery of the opening by the harness legs clearly disturbed the otherwise nearly homogeneous membrane stress distribution. In the horizontal plane, the mouth or opening was lobed, reducing its diameter by as much as 15%. In the plane tangent to the surface of the envelope at the harness attachment point, the opening was scalloped. This type of distortion was present to varying degrees on all models. Figure 9 presents a sketch of this distortion.

R_2-Perp Method: The r_2-perp method was used for only one model. It was immediately obvious by visual examination during suspended testing that this modelling method was not acceptable. The model

15

profile was prolate, appearing nearly conical from the apex to at least θ = 50 degrees. The model also showed envelope distortion in the mouth area similar to that observed in all other models.

R_2-Radius Method: The r_2-radius method was used for all subsequent models. The shape of these models compared favorably to the ideal profile, and, on the basis of visual comparison, this modelling method was judged superior to the other two. The distortion in the mouth area remained, however.

Photogrammetric Profile Comparison

Model #6 was a 12-gore, 5 kilogram model constructed using the r_2-radius method. This model most closely resembled the ideal shape when compared visually with the silhouette. Therefore, this model was further evaluated using the more quantitative photogrammetric method. From the apex to about θ = 100 degrees, the fidelity of the model with respect to the profile was excellent. The harness affected the shape of the envelope at values of θ > 100 degrees. As with all models, the cross-sectional shape and the opening were lobed rather than circular, and the opening was scalloped in the plane tangent to the envelope at the harness attachment point. The data from the photogrammetric profile comparison test are shown in Figure 10.

Capacity Testing

The capacities of the five 5 kg models were determined. Values were generally less than predicted, most probably because of the distortion of the envelope caused by the harness. In all models, point loading of the periphery of the opening tended to reduce its diameter, which tended to reduce the volume of the envelope. Also, the cross-sectional shape of all models was lobed rather than circular, which reduced the cross-sectional area and therefore the volume of the envelope.

Model #6 most closely resembled the true theoretical shape. The capacity of this 5 kg model was determined during suspended testing to be 4560 mL, or 0.912 of the design value of 5000 mL. As a result, the inverse of this value, 1.097, served as a volume correction coefficient for this type of model.

Bulk and Mass Comparison Testing

Bulk and mass of the proof-of-concept model (Model #7) and the commercially available lift device are presented in Table IV. The proof-of-concept model has less than 20% of the bulk and less than 10% of the weight of the commercial version. It should be noted, however, that a small plastic dump valve is installed in the apex of the commercial model to allow venting the bag under load. The proof-of-concept model did not have this feature, which would have increased both its weight and volume slightly.

16

Underwater Testing

Lead weights provided simulated loads for underwater testing. Values given for the weights are estimates provided by the manufacturers.

Model #1

Test #1: Ascent with 0.9 kg (2 lbs) was stable. Acceleration was noted as the model rose and the air in the envelope expanded to provide greater buoyancy. Changes in shape due to the expanding air and increasing profile drag were noted, but did not adversely affect stability. Stability on the surface was good in both quiet and intentionally disturbed water.

Test #2: With a load of 4.5 kg (10 lbs), ascent was stable and, after an initial acceleration, the velocity seemed constant. No deformations of the envelope were noted. Stability on the surface was good, although the model became fully submerged more readily in disturbed water because of its heavier load.

Test #3: When released with a fully inflated envelope and a load of 0.9 kg (2 lbs), acceleration was rapid and the model followed a helical path to the surface. Air was continuously vented from the opening during ascent. At the surface the model was stable, and although the envelope was only 70% to 80% full, buoyancy was adequate to keep the load afloat.

Model #6

Test #1: This model performed much like Model #1. However, this test was conducted with Model #6 ten times to evaluate the changes in envelope shape during ascent: Before lifting from the bottom of the pool the envelope was elongated, with a small bubble of air trapped at the apex. When buoyancy became adequate, the model left the bottom. As the velocity increased, the apex area flattened and increased the profile diameter, but the size of the opening was relatively unaffected. Finally the opening began to expand. Before expansion could be completed and the shape fully developed, the model reached the surface and assumed a steady state configuration with the envelope about half full.

Test #2: Model #6 was slightly larger than Model #1, so 5.0 kg (11 lbs) was required to load it to near-maximum capacity. During the test, this model performed much like Model #1.

Test #3: The performance of Model #6 during this test was not substantially different from the performance of Model #1.

Model #7

Performance of this model with a submaximal load (22.8 kg) was as expected. Inflation was easy to perform and ascent was smooth. The model was stable on the surface with the amount of air required to

initiate ascent. The model was also stable when fully inflated on the surface, both in quiet and intentionally disturbed water.

CONCLUSIONS

Several models of an advanced underwater lift device have been designed, constructed, and tested, including a proof-of-concept model with a capacity of 50 kg. The models exhibit significantly improved characteristics compared to commercially available designs.

It has been shown that weight and bulk of an underwater lift device can be substantially reduced by modelling the device after a pendant drop, and by using a dual membrane envelope. In one design of 50 kg capacity, bulk was reduced to less than 20% and weight to less than 10% of the same properties for a commercially available design of equivalent lifting capacity.

Although the shape was designed to exhibit a uniform membrane stress distribution, some departures from the theoretical shape indicate some degree of nonhomogeneous stress distribution. These include the scalloping at the envelope/harness interface and the lobed cross-sectional shape noted at the opening, and through any plane perpendicular to the axis of symmetry near the opening. A factor in the amount of deformation seems to be the number of gores and harness legs used to construct the device. Both theory and data suggest that a design using more gores and harness legs can provide a shape closer to ideal.

The relative proximity of the 12 harness legs to each other made the 12-gore models slightly more difficult to inflate than the 6-gore models, particularly in smaller sizes (5 kg). This effect was much less noticeable with the larger 12-gore model (50 kg), and should not present significant problems in units of this size or larger.

The use of staples to bond the inner and outer membranes together at the opening of the underwater lift devices was less effective than the use of double sided masking tape.

Overall, the use of a pendant drop shape plus a dual membrane envelope has been shown to significantly advance the design of an underwater lift device. Areas for improvement have been noted, and recommendations for further study are outlined below.

RECOMMENDATIONS

The materials used in this study were selected arbitrarily. A comprehensive trade study should be performed to identify more appropriate materials for use in the field.

The tensile moduli of the selected materials need to be determined with better accuracy.

18

Membrane stress on the surface of the envelope may be quantified in future testing using strain gauges designed for fabric.

Only 6- and 12-gore designs were used in this study. Other values that could provide better stress distributions or that could be easier to use could be investigated.

A more suitable method of bonding the inner membrane to the outer membrane at the opening of the envelope needs to be developed for use in the field.

The combination of conventional envelope materials (polymer-coated fabrics) and the pendant drop geometry could provide a less complex (although less effective) solution to bulk and weight reduction. This could be investigated. Similarly, application of the dual membrane envelope concept to conventional envelope geometries could also be pursued.
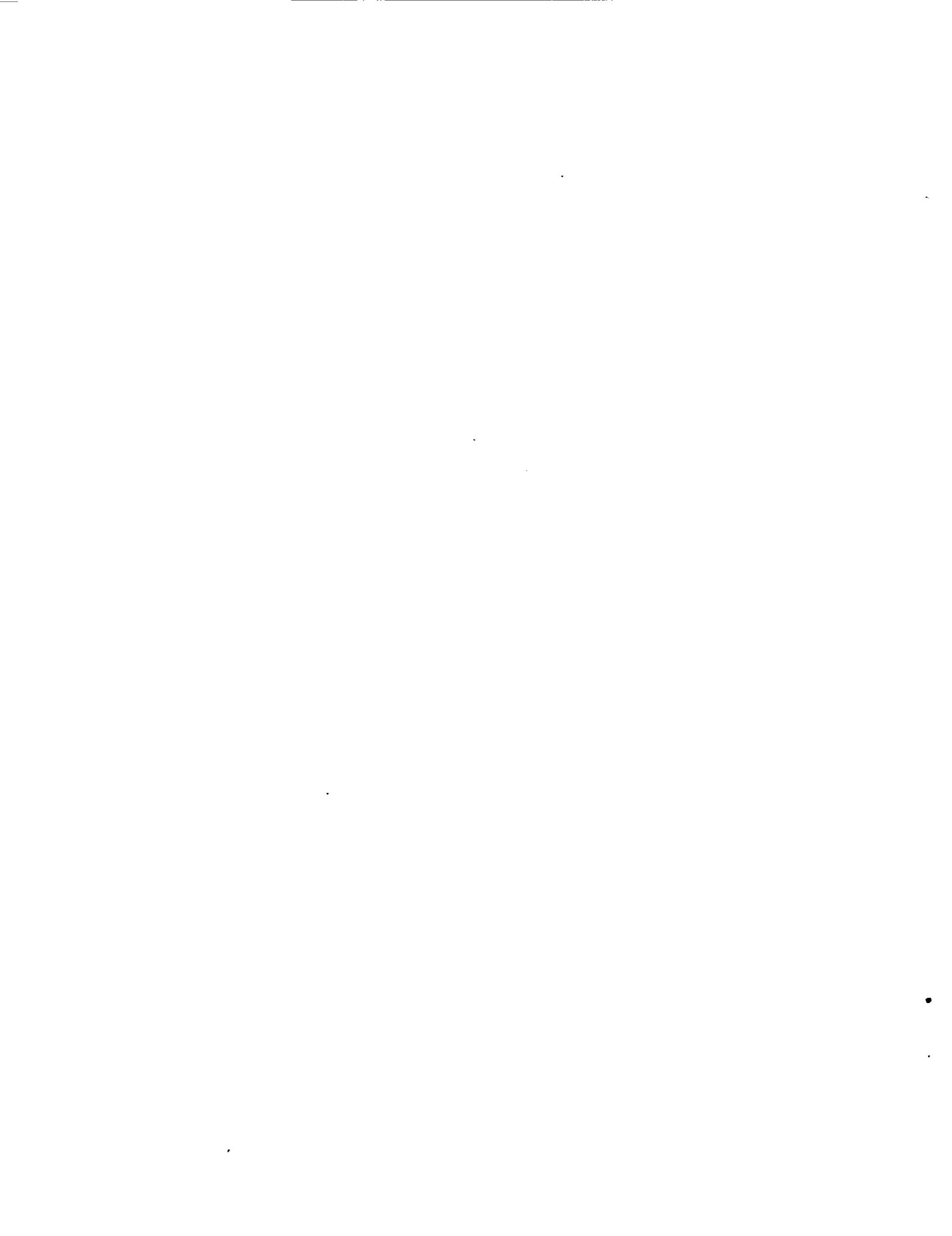
Table I. Dimensionless parameters of a pendant drop having a shape factor log(B)=-0.24 (4).

ANGLE =Θ	ARC LENGTH = S	X	Z	AREA	VOLUME
5	5.02324E-02	5.01687E-02	2.19076E-03	7.92215E-03	8.66629E-06
10	1.00560E-01	1.00050E-01	8.75879E-03	3.16882E-02	1.38042E-04
15	1.51079E-01	1.49356E-01	1.96914E-02	7.12969E-02	6.93648E-04
20	2.01889E-01	1.97798E-01	3.49677E-02	1.26746E-01	2.16945E-03
25	2.53091E-01	2.45086E-01	5.45587E-02	1.98033E-01	5.22549E-03
30	3.04793E-01	2.90930E-01	7.84281E-02	2.85152E-01	1.06576E-02
35	3.57109E-01	3.35036E-01	1.06533E-01	3.88100E-01	1.93601E-02
40	4.10161E-01	3.77108E-01	1.38823E-01	5.06870E-01	3.22825E-02
45	4.64083E-01	4.16846E-01	1.75245E-01	6.41456E-01	5.03826E-02
50	5.19022E-01	4.53945E-01	2.15743E-01	7.91853E-01	7.45758E-02
55	5.75144E-01	4.88092E-01	2.60260E-01	9.58061E-01	1.05684E-01
60	6.32639E-01	5.18965E-01	3.08741E-01	1.14009E+00	1.44389E-01
65	6.91726E-01	5.46228E-01	3.61141E-01	1.33796E+00	1.91180E-01
70	7.52668E-01	5.69529E-01	4.17431E-01	1.55173E+00	2.46321E-01
75	8.15783E-01	5.88486E-01	4.77611E-01	1.78152E+00	3.09814E-01
80	8.81472E-01	6.02679E-01	5.41727E-01	2.02753E+00	3.81384E-01
85	9.50257E-01	6.11630E-01	6.09905E-01	2.29015E+00	4.60475E-01
90	1.02285E+00	6.14764E-01	6.82409E-01	2.57008E+00	5.46269E-01
95	1.10029E+00	6.11348E-01	7.59746E-01	2.86864E+00	6.37752E-01
100	1.18420E+00	6.00344E-01	8.42904E-01	3.18837E+00	7.33841E-01
105	1.27748E+00	5.80079E-01	9.33926E-01	3.53468E+00	8.33697E-01
110	1.38647E+00	5.47169E-01	1.03779E+00	3.92117E+00	9.37689E-01
115	1.53332E+00	4.90549E-01	1.17324E+00	4.40083E+00	1.05287E+00
*1.17417E+02		4.13273E-01	1.32768E+00	4.89182E+00	1.15250E+00
115	1.85557E+00	3.46227E-01	1.46134E+00	5.24821E+00	1.21303E+00
110	1.95657E+00	3.07168E-01	1.55445E+00	5.45510E+00	1.24414E+00
105	2.02254E+00	2.87209E-01	1.61730E+00	5.57810E+00	1.26153E+00
100	2.07575E+00	2.75636E-01	1.66922E+00	5.67206E+00	1.27441E+00
95	2.12273E+00	2.69476E-01	1.71577E+00	5.75240E+00	1.28525E+00
90	2.16667E+00	2.67546E-01	1.75966E+00	5.82644E+00	1.29516E+00
85	2.20966E+00	2.69420E-01	1.80260E+00	5.89889E+00	1.30486E+00
80	2.25344E+00	2.75145E-01	1.84599E+00	5.97370E+00	1.31495E+00
75	2.29984E+00	2.85211E-01	1.89127E+00	6.05529E+00	1.32609E+00
70	2.35121E+00	3.00696E-01	1.94023E+00	6.14972E+00	1.33926E+00
65	2.41119E+00	3.23718E-01	1.99559E+00	6.26723E+00	1.35617E+00
60	2.48662E+00	3.58673E-01	2.06242E+00	6.42872E+00	1.38054E+00
55	2.59409E+00	4.16684E-01	2.15283E+00	6.69004E+00	1.42311E+00
50	2.80291E+00	5.44892E-01	2.31758E+00	7.31930E+00	1.54251E+00
45	3.75348E+00	1.19001E+00	3.01546E+00	1.24761E+01	3.23995E+00
40	4.19386E+00	1.51316E+00	3.31443E+00	1.62099E+01	4.95194E+00
35	4.48056E+00	1.74021E+00	3.48934E+00	1.91379E+01	6.40223E+00
30	4.71535E+00	1.93804E+00	3.61566E+00	2.18497E+01	7.74123E+00
25	4.92422E+00	2.12318E+00	3.71220E+00	2.45136E+01	8.98854E+00
20	5.11876E+00	2.30283E+00	3.78669E+00	2.72180E+01	1.01315E+01
15	5.30580E+00	2.48115E+00	3.84295E+00	3.00286E+01	1.11394E+01
10	5.49029E+00	2.66120E+00	3.88287E+00	3.30087E+01	1.19648E+01
5	5.67664E+00	2.84591E+00	3.90716E+00	3.62326E+01	1.25392E+01
0	5.86971E+00	3.03873E+00	3.91551E+00	3.98018E+01	1.27614E+01

Table II. Pertinent specifications of MIL-C-7020G nylon parachute cloth (6).

Property	Type I	Type II	Type III
Weight, Maximum (ou/yd)	1.1	1.6	1.6
Thickness, Maximum (in)	0.003	0.004	0.004
Tensile Strength, Minimum (lbs/in)			
Warp	42	50	50
Fill	42	50	50
Elongation, Minimum Both Directions (%)	20	20	20
Tearing Strength, Minimum (lbs)			
Warp	5 +/- 1	5	4
Fill	5	5	4

Table III. Pertinent specifications of MIL-C-5040G braided nylon cord (7).

Property	Type IA	Type IIA
Breaking Strength, Minimum (lbs)	100	225
Elongation, Minimum (%)	30	30
Length Per Pound Minimum (ft)	1050	495

Table IV. Bulk and weight of the proof-of-concept model vs. the control model of the same capacity.

	Bulk (Volume) cm^3	Weight (Mass) gms
Model #7 (50 kg) Proof-of-concept model	735	114
J. W. Automarine (50 kg) Commercial control	4,129	1,351

Table V. Characteristics of some aerospace materials potentially useful in the design of underwater lift devices (3).

Characteristic	Dimensions	Silk	Cotton	Rayon	Nylon	Dacron	Nomex	Kevlar 29
Staple length	Inch	400-1300 yds	½-2½	Continuous	Continuous	Continuous	Continuous	Continuous
Tensile strength	lb/in^2	–	–	–	118,000	120,000	90,000	370,000
Tenacity	Gr/Denier	3.8-5.2	2.1-6.3	1.5-5.0	6-9	6-9	5	20-22
Specification weight	Gr/Cm^3	1.34	1.52	1.5	1.14	1.38	1.38	1.44
Ultimate elongation	%	13-31	3-7	15-25	25-40	12-20	16	3-5
Zero strength (melting point)	°F	302(D)	450(D)	350-450	480	485	800	850
50% strength retention	°F	280	300	–	330	350	500	550
Minium yarn size	Denier	11/13	15	20	20	20	200	50
Filament diameter	Inch	0.0005	<0.001	0.0005	0.001	0.001	–	0.0005
Wet strength	%	75-95	110-130	45-55	85-90	95	65	100
Resistance to								
Ultraviolet rays		P	G	P	P	G	G	D
Storage, aging		G	G	G	E	E	E	G
Fungus, bacteria		P	P	P	G	G	G	G
Flame		P	Burns	Burns	G	G	E	G

NOTE: P = poor, G = good, E = excellent
(D) decomposes

Pendant
Drops

Heavy
Liquid

Light | Liquid

Light
Liquid

Heavy | Liquid

Curvature at
apex = 1/b

x

Θ

s

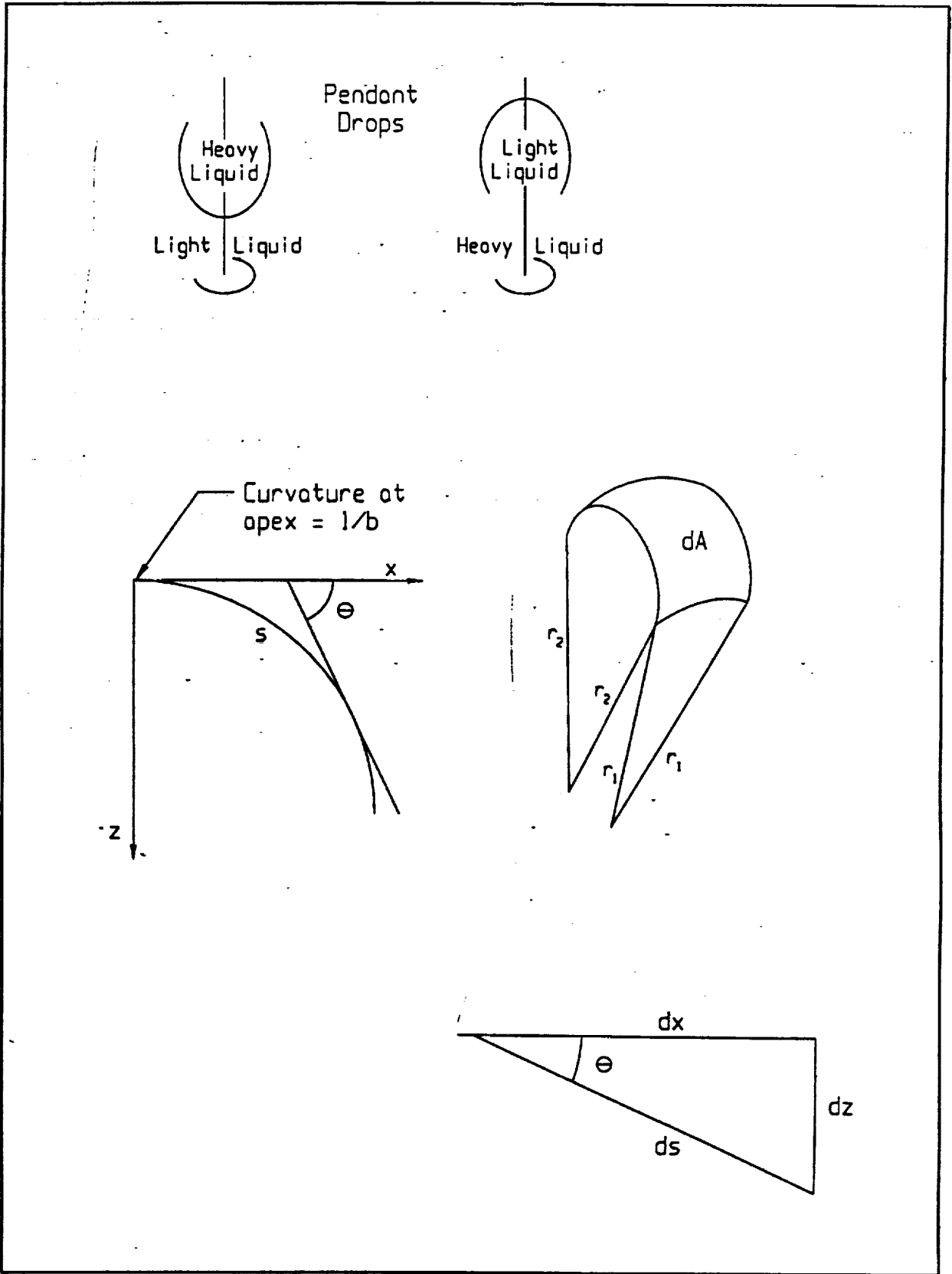$\cdot$z

dA

r_2

r_2

r_1

r_1

dx

Θ

dz

ds

Figure 1. General notation for pendant drops (4).
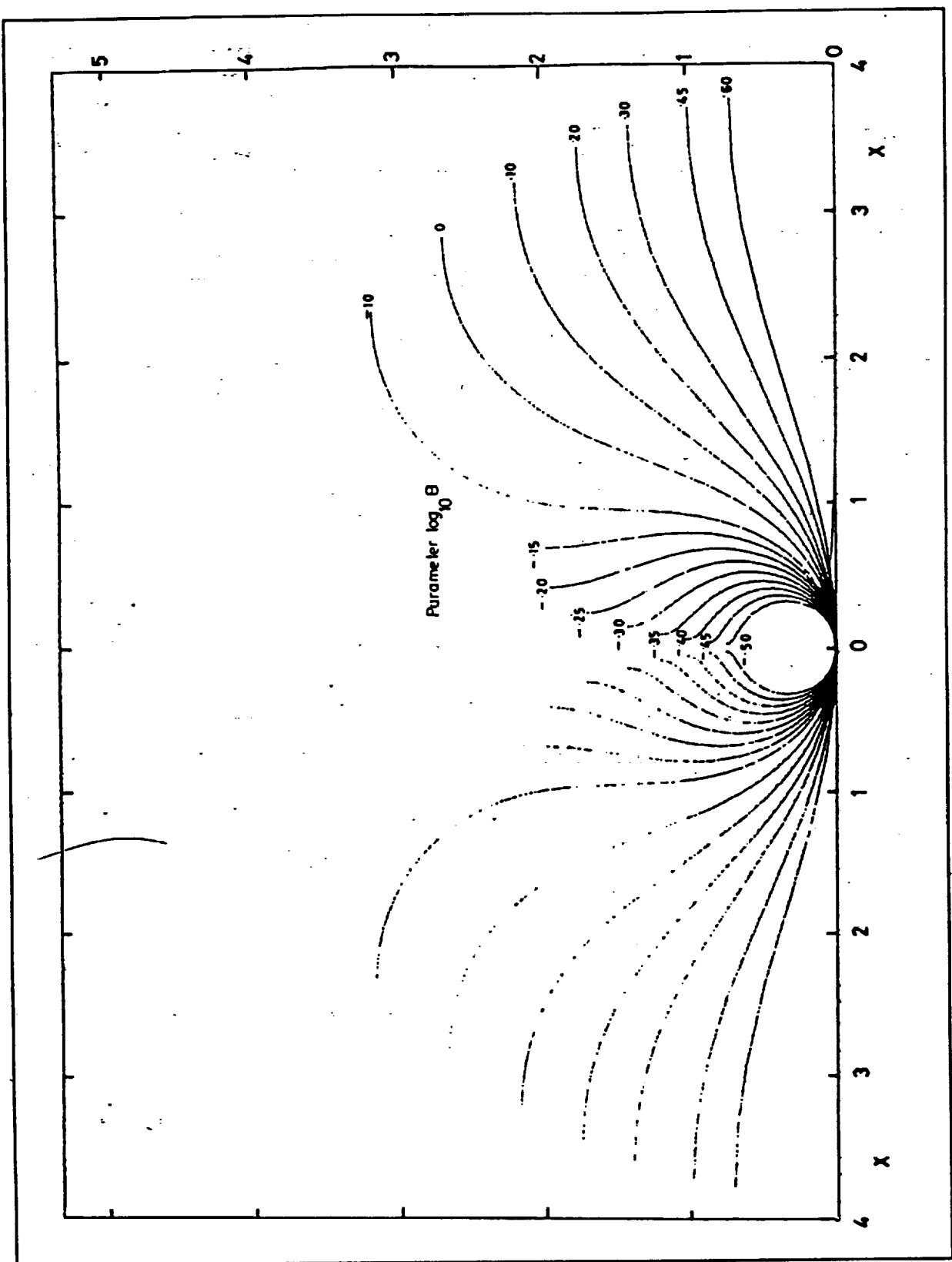
Figure 2. Profiles of pendant drops with respect to the dimensionless shape factor log(B) (4).
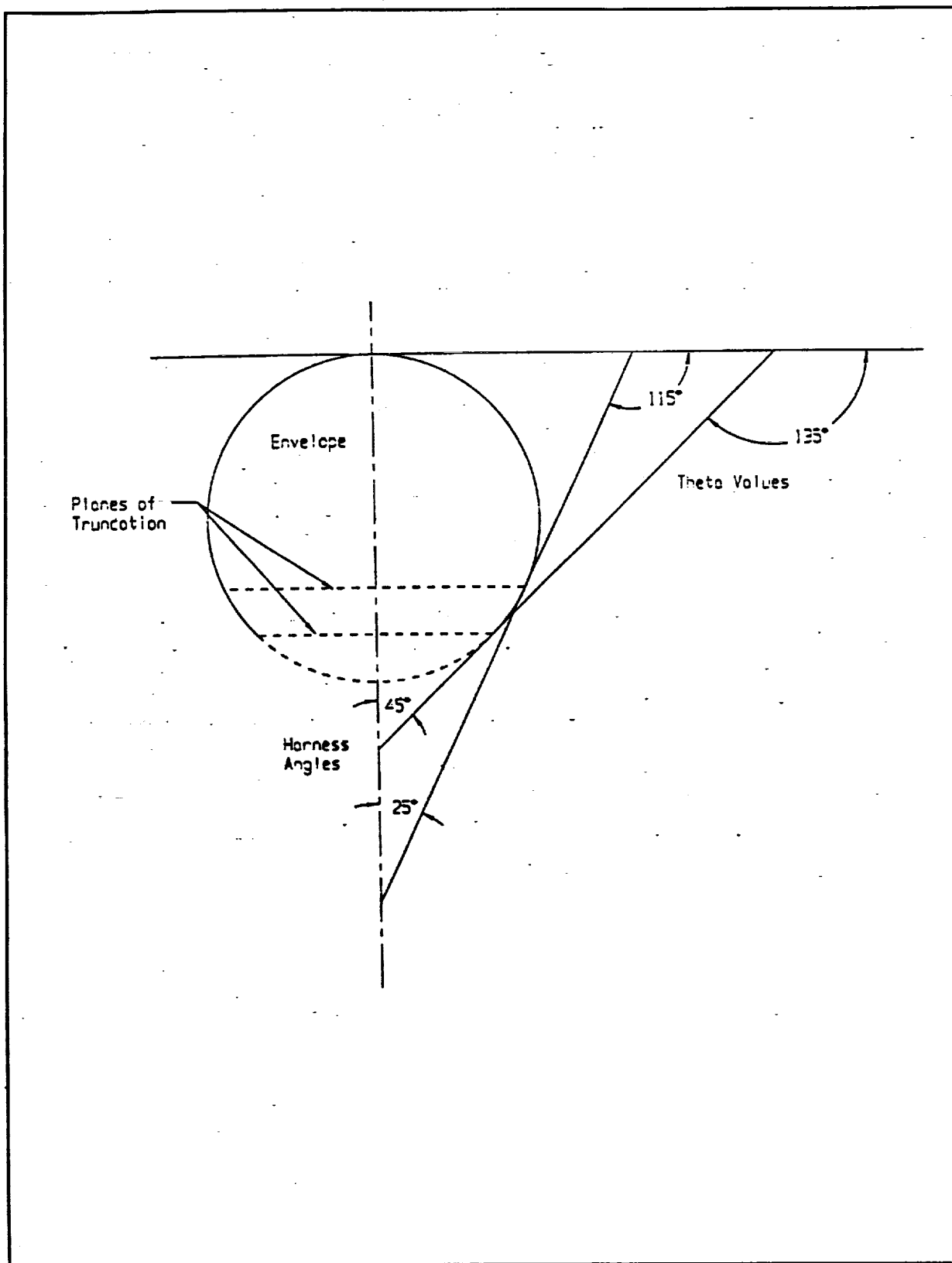
Figure 3. Relationship between the selected plane of truncation and the resulting harness angle

Apex

s

s

$\frac{2\pi}{n}$ rad

x

x

Secant line "sl"
in plane of x and
in plane of r_2

Arc in plane of r_2

Arc in plane of x

r_2
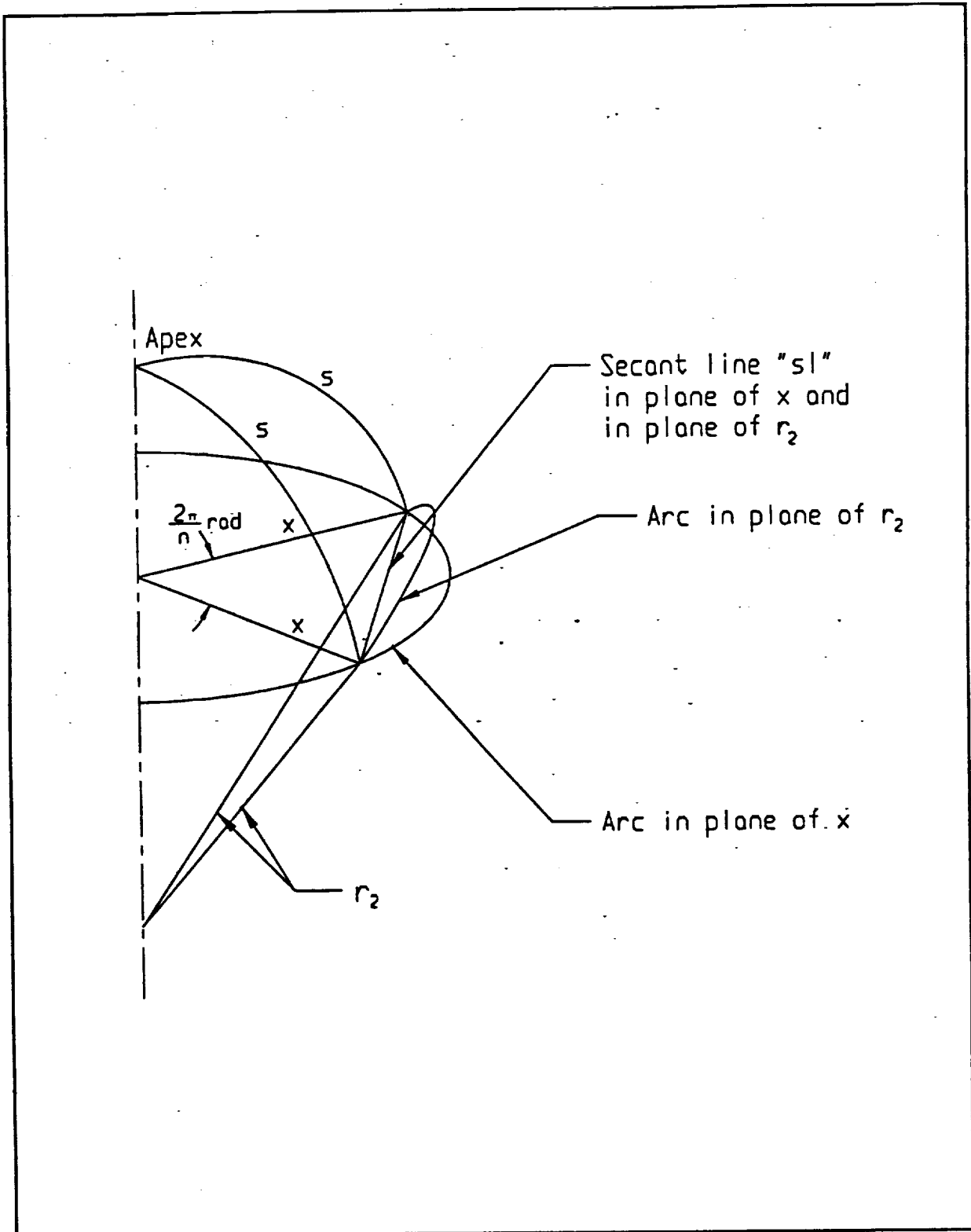
Figure 4. Parameters for developing gore patterns. The plane created by r_2 through $d\alpha$ is orthogonal to the surface of the drop. The plane created by x through any angle $2\pi/n$ is orthogonal to the axis of symmetry.
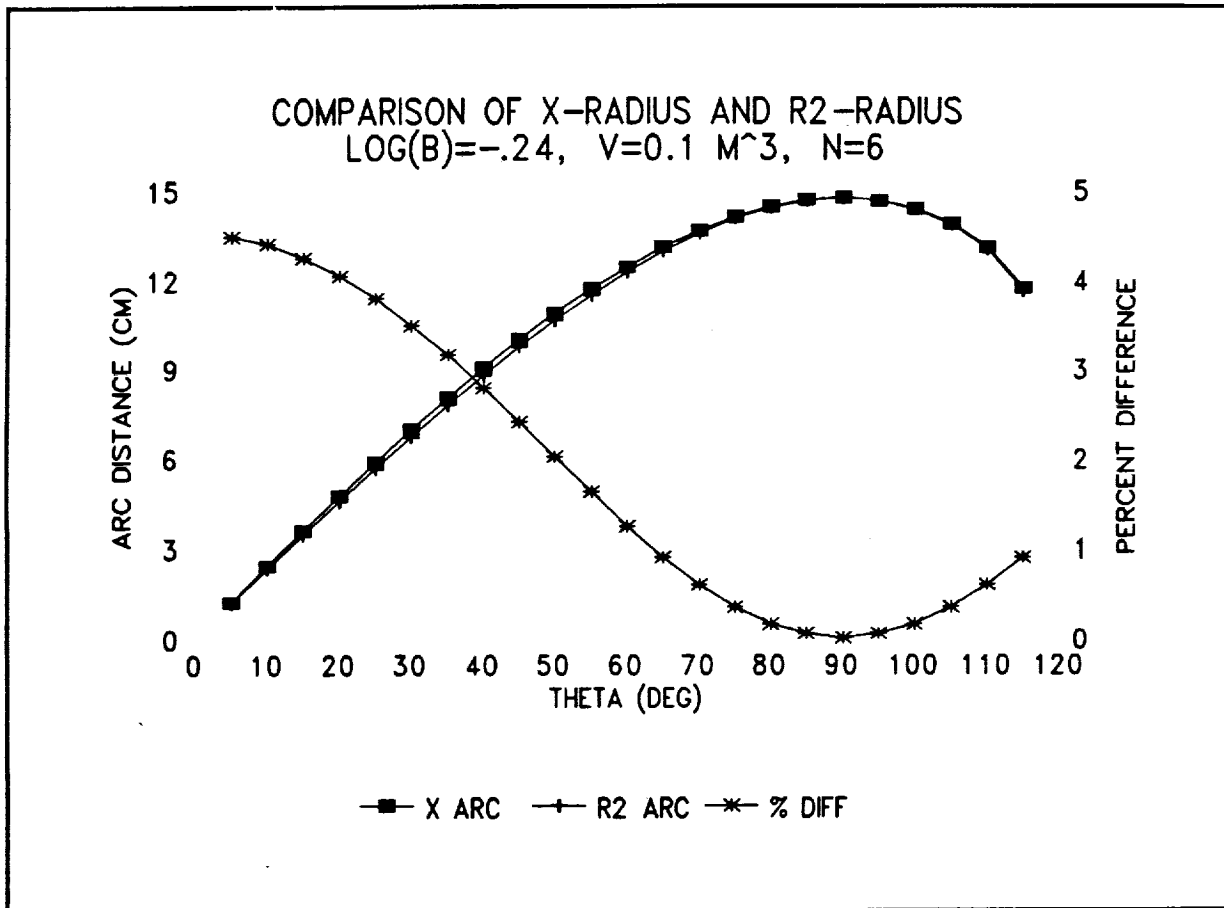
Figure 5. Comparison of the radii used to create gores using the x-radius and r_2-radius modelling methods. The greatest percent difference occurs at the apex, the greatest absolute difference at θ = 45.
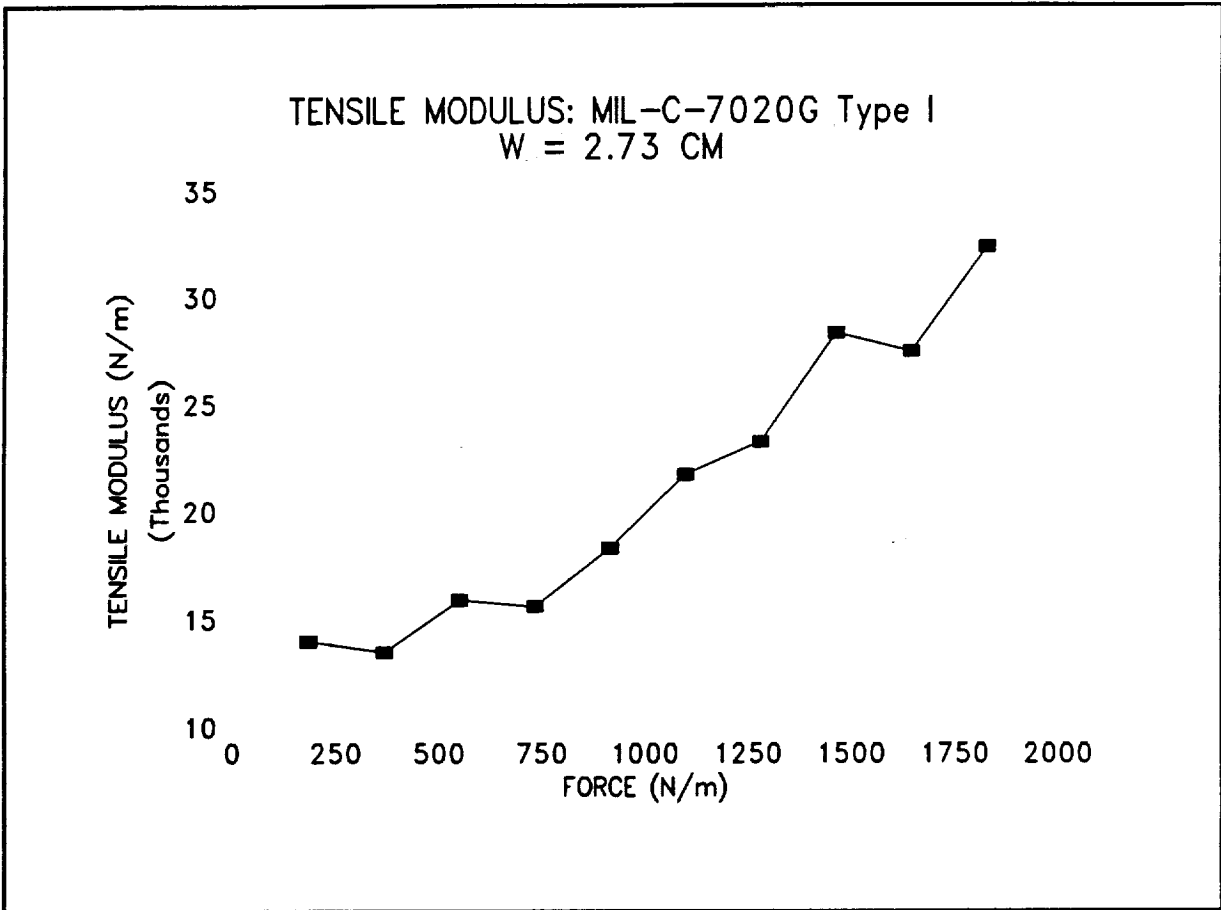
Figure 6. Tensile modulus of the membrane material: MIL-C-7020G Type I parachute fabric.
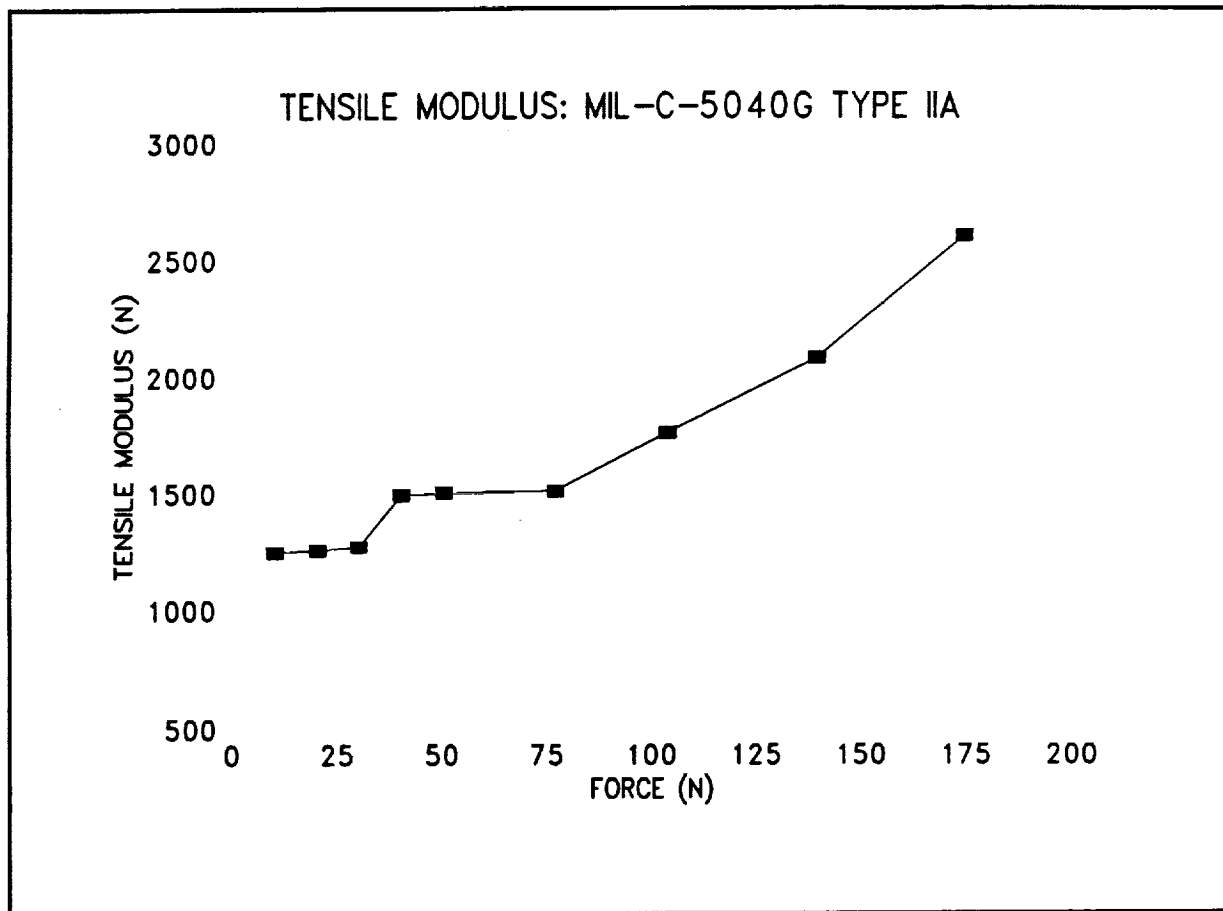
Figure 7. Tensile modulus of the harness material: MIL-C-5040G Type IIA parachute cord.
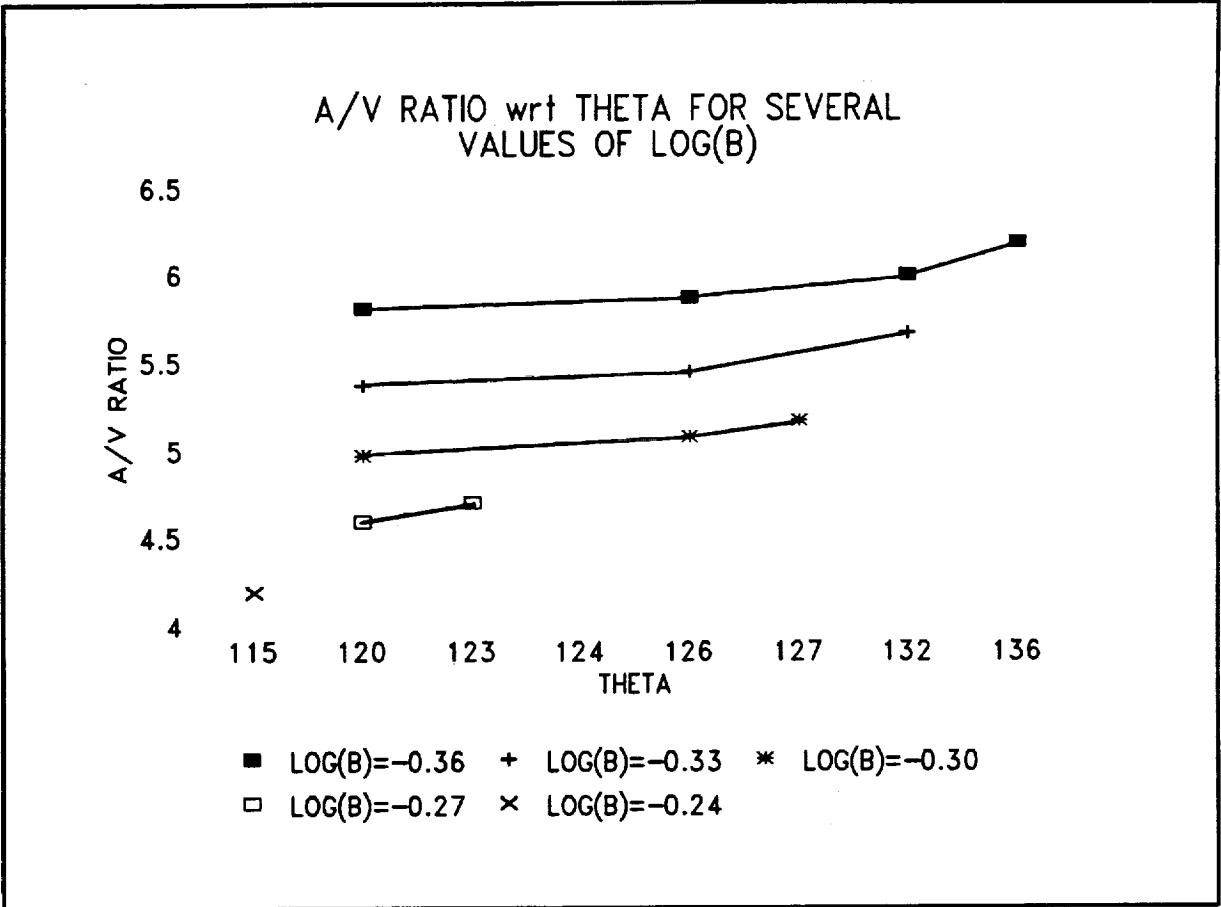
Figure 8. Dimensionless surface-to-volume ratios computed from the data in reference 4 for values of θ and log(B).
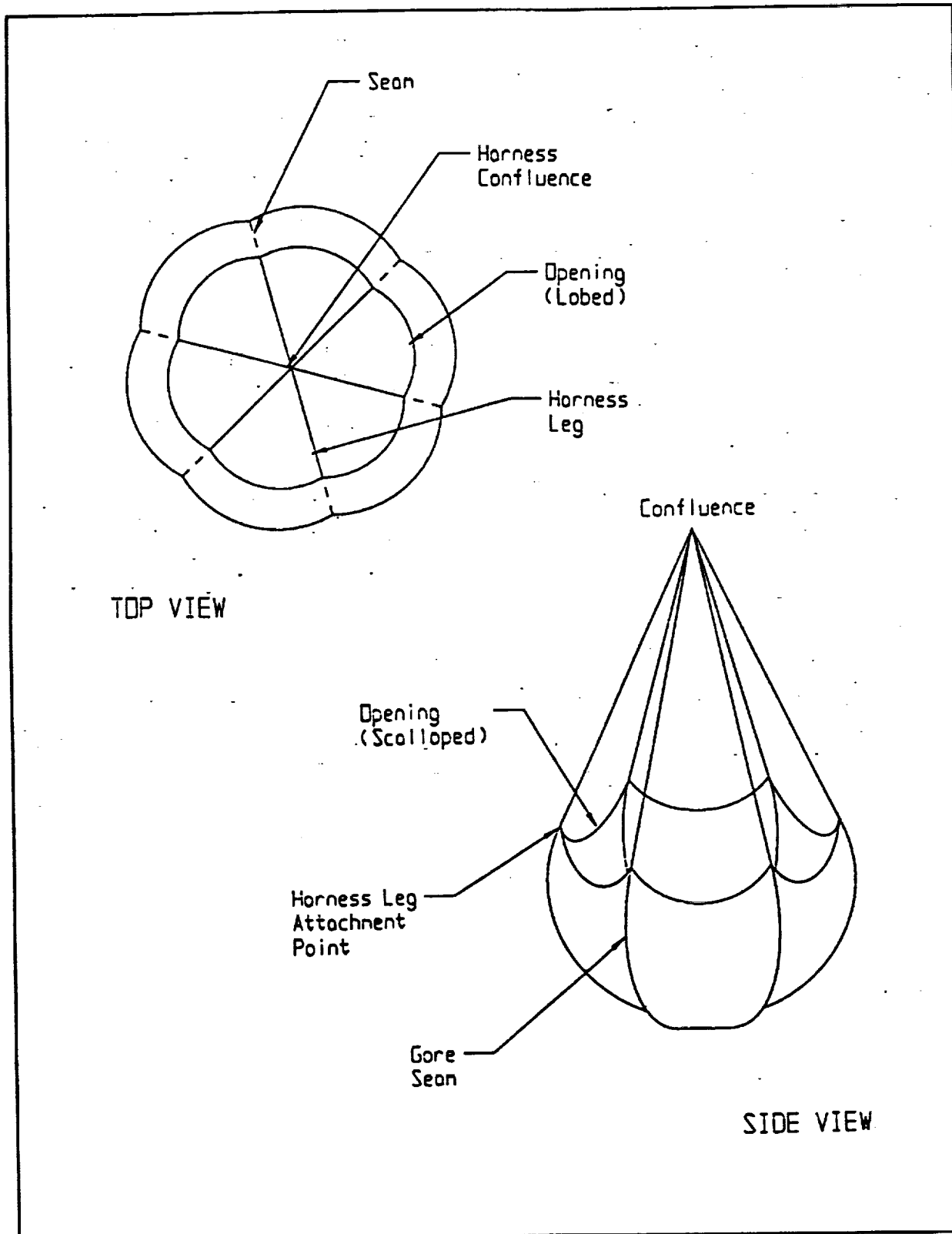
Figure 9. Distortion at the opening of the envelope membrane under load. The cross-section is lobed. Scalloping is obvious is the vertical planes.
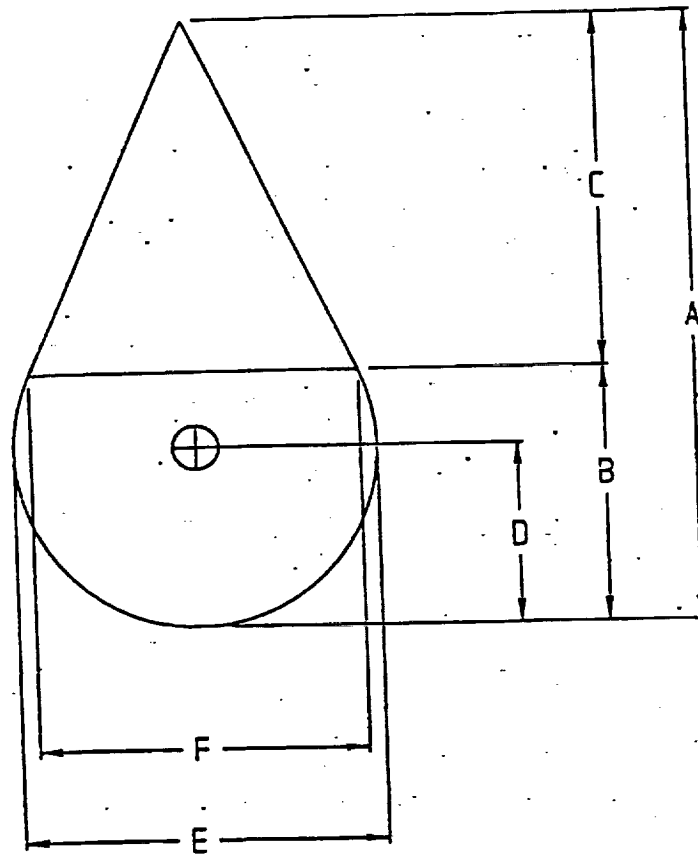
Dimension	Model #6 (View #1)	Model #6 (View #2)
A	1.03	1.02
B	0.99	1.01
C	1.05	1.04
D	0.99	0.99
E	0.99	0.99
F	0.93	*

*Data could not be obtained. View of the opening was obscured by excess inner membrane material projecting from the opening.

Figure 10. Photogrammetry data from Model #6. Each value given is the ratio of the dimension on the model to the corresponding dimension on the silhouette. View#1 and View #2 differ by a 15 degree rotation of the model about the axis of symmetry

REFERENCES

1. Flanagan, D.T., unpublished results, 1988.

2. National Space Transportation System Reference Guide, Volume 1, National Aeronautics and Space Administration, June 1988.

3. Knacke, T.W., Parachute Recovery Systems Design Manual, Naval Weapons Center, China Lake, California, NWC-TP-6575, March 1991.

4. Hartland, S., and Hartley, R. W., Axisymmetric Fluid-Liquid Interfaces, Elsevier Scientific Publishing Company, NY, 1976.

5. Poynter, D., The Parachute Manual, Volume II, Parapublishing Company, Santa Barbara, California, 1991.

6. MIL-C-7020G, Cloth, Parachute, Nylon., 22 August 1978., Available from the Superintendent of Documents, U.S. Government Printing Office, Washington, D.C. 20402.

7. MIL-C-5040G, Cord, Fibrous, Nylon., 30 June 1987., Available from the Superintendent of Documents, U.S. Government Printing Office, Washington, D.C. 20402.
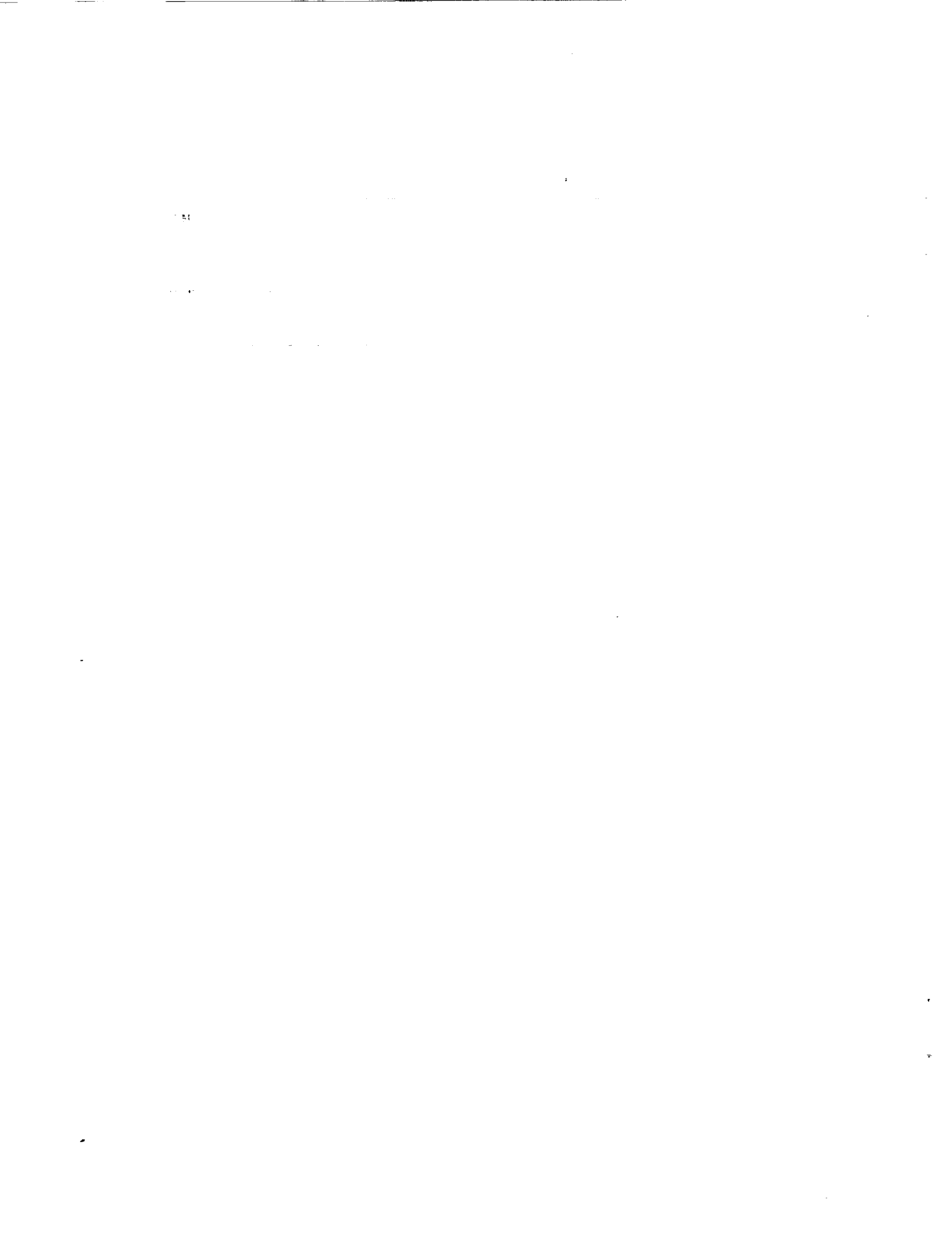
APPENDIX A

Model Summary

Model #1: Model #1 was a 6-gore model of 5 kg capacity fabricated using the x-radius method of modelling. No sewing take-up allowance was incorporated. The tensile modulus for the membrane stress was arbitrarily set at 17,777 N/m. No apex cap was installed. The length of the harness was marked while the model was under load, and the harness legs tied together at that point using a waxed cord.

During visual evaluation the model appeared slightly oblate. Volume was 4150 mL compared to the theoretical capacity of 5000 mL.

Model #2: Model #2 was a 6-gore model of a nominal 5 kg capacity constructed using the x-radius modelling method. In this model, a 1.02 correction coefficient was applied to dimensions along the gore axis. No correction was applied to gore width dimensions. The intent was to compensate for the oblate shape seen in Model #1. Again the tensile modulus for the membrane stress was arbitrarily set at 17,777 N/m, and the length of the harness legs was determined under load.

During visual evaluation this model was decidedly prolate, and held only 4100 mL of the theoretical 5000 mL capacity.

Model #3: Model #3 was a 5 kg, 6-gore model constructed using the x-radius modelling method. The tensile modulus was set at 17,777 N/m and an arbitrary 1.04 sewing take-up correction factor was applied to all gore dimensions. An apex cap about 5 cm in diameter was installed to control dimensional instability in the nose area where the gore seams met. Harness leg lengths were determined under load.

The oblate shape seen in Model #1 was also present in this model. capacity was 4930 mL of the theoretical 5000 mL.

Model #4: Model #4 was a 5 kg, 6-gore model constructed using the r_2-perp method. The tensile modulus was set at 17,777 N/m and an arbitrary 1.04 sewing take-up coefficient was applied to all gore dimensions. An apex cap was installed and harness leg lengths were determined under load.

The shape of this model was conical at the apex area. Volume was 4720 of the theoretical 5000 mL.

Model #5: Model #5 was a 6-gore, 25 kg capacity model constructed using the r_2-radius method. A 1.04 sewing take-up correction coefficient was applied to all gore dimensions. Tensile modulus was set at 17,777 N/m and harness leg lengths determined under load. An apex cap was installed.

Visual evaluation showed the profile of this model to be comparable to its silhouette. Deformation in the area of the opening (reduced diameter, a lobed cross-section and scalloping of the edges between harness legs), noted in all models, was particularly evident in this model. The volume of water it held was not determined.

Model #6: Model #6 was a 5 kg, 12-gore model based on the r_2-radius method. Tensile modulus was determined by the computer program on the basis of the tensile modulus testing which had been performed. A 1.02 sewing correction coefficient, also based on testing, was applied to all gore dimensions. An apex cap was installed. The harness leg length was determined under load.

Visual comparison of the profile of this model with its silhouette was excellent. Distortion in the harness attachment area were reduced. Volume was 4560 mL of the theoretical 5000 mL.

Model #7: Model #7 was a 50 kg proof-of-concept model having 12 gores fabricated per the r_2-radius method. Corrections for stress and sewing take-up on membrane and harness materials were performed on the basis of materials testing. A volume correction coefficient of 1.097 was applied by the computer program to the input volume. An apex cap was installed. Harness legs were precut to the correct length and then installed.

The suspended model was visually evaluated, but no silhouette existed for this size model. Distortions in the opening area seen on Model #5 were greatly reduced. The capacity of this model was not determined. Weight and bulk were recorded.

37

APPENDIX B

MATERIALS AND METHODS

Material Selection

An extensive selection of candidate materials exists for application to the design of underwater lift devices. Many are currently used in aerospace applications such as parachute recovery systems, where low bulk and high strength are important. These materials include nylon, dacron, kevlar, nomex, and spectra, as well as hybrid materials woven from combinations of these materials. Characteristics of a few of these materials are presented in Table V.

Time constraints did not permit a detailed comprehensive trade study of all candidate materials. Selection was based primarily on the basis of the investigators' knowledge. Considerations included weight, thickness, strength, expense, and availability.

Material Testing

Tensile Modulus Testing

Outer Membrane Material

A strip of fabric about 5 cm wide was cut to a length of about one meter. Each end was mounted firmly in clamps with rubber-lined jaws 2.73 cm wide. The fabric was aligned with warp yarns parallel to the direction of pull. One clamp was mounted on an overhead beam and the other attached to a lightweight bucket that was allowed to hang freely. Two marks 76 cm apart were made on the fabric. Weights were sequentially added to the bucket in 5 N increments (equivalent to .510 kg mass) to a total of 50 N. The distance between the marks was recorded one minute after each weight was added. The delay permitted equilibrium to be established.

The weight provided the stress distributed across the width of the fabric in N/m, and the original length in meters and resulting elongation in meters were directly measured.

Harness Material

The harness material was tested similarly. Loops were fingertrapped (5) in each end of a coupon about one meter long. One end was fixed to an overhead beam and the free end to the bucket. Two marks were made 87 centimeters apart on the coupon. Weights of several sizes were added sequentially to the weight bucket to a maximum of 174 N, and, after a one minute delay to allow equilibrium to be established, the amount of elongation was recorded.

Functions relating moduli and stress were generated for both membrane and harness material through regression analysis using Cricket software on a Macintosh SE computer.

Sewing Take-up Testing

The fabric pieces of the outer membrane were joined using a simple 301 machine lockstitch (5). The fabrication take-up of this stitch was documented using four long coupons of fabric. First, a doubled piece of outer membrane fabric was laid out and gently stretched to remove wrinkles. Two marks 80 cm apart were made on the fabric, and a seam of the selected type was sewn along the two layers between the two marks. After sewing, the fabric was again stretched, only enough to remove wrinkles, and the distance between the marks measured.

Computer Design Program

The interactive computer design program was written in generic BASIC (BASICA or GWBASIC) on a 386-based personal computer.

Model Construction

Raw materials for the models were obtained from ParaGear Equipment Company, Skokie, Illinois, 60076. Part numbers given below are from ParaGear Catalog #55 (1990-1991).

The computer program was used to generate construction data. A gore pattern was drawn on light cardboard stock and traced onto the membrane material (P/N W9190). Gores were block cut in that the gore axis was oriented parallel to the warp or fill of the fabric. A seam allowance of roughly 3/4" was allowed in cutting out the gores. The gores were sewn together on a common Sears Kenmore household sewing machine with a 301 lockstitch using nylon "E" thread (P/N T-1009) at a machine setting of six stitches per inch (spi). An apex cap of adhesive-backed membrane material (P/N W901) was installed on many of the 5 kg models to control the dimensional instability that occurred where the seams met at the apex. Apex caps without the adhesive backing were sewn onto the apices of the envelopes of the two larger models for the same purpose. Harness legs of Type IA material (P/N W9660) were attached using the same stitch. A 304 lockstitch (single throw zig-zag) was used at six spi to attach harness legs of Type IIA material (P/N W9670 with core lines removed). In all models the number of harness legs equaled the number of gores. A excellent discussion of fabric joints, stitch types, and fabrication techniques applicable to the types of materials used in this study can be found in reference 5.

For smaller models, harness legs were evenly cut to excess length after installation, gathered, and knotted at the most distal point. During suspended testing (that is, under load) the correct length was marked, and either another overhand knot was tied, or the

harness was otherwise gathered together at that point by tying a length of heavy waxed cord (P/N T1050) around the harness legs.

On the 50 kg proof-of-concept model, small loops were fingertrapped in the confluence end of each harness leg before installation. The required length, determined by the computer design program, was then marked on each harness leg, and the leg was then installed using the 304 lockstitch as noted above. The confluence was formed by threading the fingertrapped loops onto a #5 Maillon Rapide rapid connector link (P/N H358-5).

For most testing, the inner membranes of the models were generally not fastened to the outer membranes. For underwater testing, however, the membranes were either taped together using double-sided masking tape or stapled together at the opening of the envelope.

Five 5 kg models, one 25 kg model, and one 50 kg model were constructed during the course of this project. The models are briefly described in Appendix A.

Model Testing

Suspended Testing

Capacity Testing

Capacities of the smaller lift devices (5 kg) were obtained by filling them to maximum capacity, then siphoning the water into a 2 L graduated cylinder as required to empty them, and noting the volume. Capacities of the two largest models were not determined.

Profile Testing

All models except Model #6 received only a subjective visual evaluation of their profile during suspended testing.

The profile of Model #6 was photogrammetrically compared to its theoretical shape. A black-on-white silhouette representing the theoretical shape was fabricated using dimensions calculated from the Z and X data for the shape factor log(B)=-0.24 (Table I). The silhouette was photographed using a Minolta X-700 35 mm camera equipped with a 210 mm telephoto lens and ASA 160 slide film. The camera-to-subject distance was adjusted so that the image filled the frame. Without disturbing the camera, the silhouette was replaced by the water filled lift bag, which was also photographed. The two slides were then projected from the same distance onto a screen where comparative measurements were taken. The ratios of each dimension measured on the projection of the model to the corresponding dimension measured on the projection of the silhouette were calculated.

Bulk and Mass Comparison Testing

The 50 kg capacity proof-of-concept lift device was weighed on a Mettler balance (P/N PM4600), and its packaged volume estimated by loosely wrapping the envelope with the harness, and measuring the resulting package with a centimeter rule (assuming a rectangular parallelopiped shape). Information was obtained similarly for a 50 kg capacity lift device manufactured by J.W. Automarine, Norfolk, England.

Underwater Testing

Three of the models were taken into a 2.6 m (8.5 ft) deep indoor pool for evaluation. Two lead ingots of approximately 11.4 kg (25 lbs) each and an assortment of lead weights normally used for scuba diving were available to provide simulated loads. Underwater photographs were taken using a disposable waterproof Kodak 35 mm camera (Fun Saver Weekend 35). The camera came preloaded with ASA 400 color print film.

Models #1 & #6

Deployment, handling, inflation and ascent characteristics were evaluated.

Test #1: Models were attached to a 0.9 kg (2 lb) mass, inflated until some small positive buoyancy was achieved, and ascent characteristics observed.

Test #2: Test #2 was identical to Test #1, but the mass to be lifted was nearer maximum capacity. Model #1 carried 4.5 kg (10 lbs) and Model #6 carried 5 kg (11 lbs).

Test #3: Ascent characteristics of the fully inflated model under a minimum load of 0.9 kg (2 lbs) were also ascertained. This test simulates a common marine salvage situation in which an object is mired in the bottom substrate, and force substantially in excess of its in-water weight is required to initiate ascent.

Model #7

The proof-of-of concept model could not be tested underwater to full capacity (50 kg) because the amount of lead mass available was not sufficient. Deployment, handling, inflation, and ascent characteristics under a submaximal load of 22.8 kg (50 lbs) were evaluated, however.

```
100    REM PENDANT DROP ULB DESIGN PROGRAM - USES R2 ARCRADIUS INSTEAD OF X
110    REM ANY BLINKING VALUES IMPLY THAT THEY EXCEED KNOWN OR TESTED RANGES.
120    SCREEN 0
130    COLOR 15,2,0
140    CLS:PRINT:PRINT:PRINT:PRINT
150    LET PI = 3.141592654#
160    COLOR 15,1,0
170    PRINT "                    PENDANT DROP UNDERWATER LIFT BAG DESIGN PROGRAM
       "
180    PRINT "                         SHAPE FACTOR: LOG(B) = -0.24
       "
190    PRINT "MEMBRANE: MIL-C-7020G TYPE I                    HARNESS: MIL-
C-5040 TYPE II":PRINT:PRINT:PRINT
200    COLOR 15,2,0
210    S=1.53332:XM=.490549:XE=.614764:Z=1.17324:A=4.40083:V=1.05287
220    THD=115:ZH=1.051986:SUMZ=2.225226:LH=1.160738:FTUH=1.02:VCD=1.097
230    YSIGH=17777:YHH=15000:RAD=PI/180:K=0:K1=0
240    COLOR 15,1,0
250    INPUT "FRESH WATER LIFTING CAPACITY (KG):  ",KG
260    COLOR 15,1,0:PRINT
270    INPUT "NUMBER OF GORES:  ",N
280    COLOR 15,1,0:PRINT
290    IF N < 6 THEN 270
300    IF N = 12 THEN 370
310    PRINT "INPUT VOLUME CORRECTION COEFFICIENT"
320    INPUT "FROM 0.90 TO 1.20 (DEFAULT IS 1.00):  ",VCD
330    COLOR 15,1,0:PRINT
340    IF VCD=0 THEN VCD=1
350    IF VCD>=.9 AND VCD=<1.2 GOTO 370
360    GOTO 310
370    PRINT "INPUT FABRICATION TAKE-UP COMPENSATION COEFFICIENT"
380    INPUT "FROM 1.00 TO 1.10. (DEFAULT IS 1.02):  ",FTU
390    COLOR 15,1,0:PRINT
400    IF FTU=0 THEN FTU=FTUH
410    IF FTU>=1 AND FTU=<1.1 GOTO 440
420    GOTO 370
430    COLOR 0,1,0:CLS
440    REM COMPUTES VOLUME BASED ON SELECTED LIFT CAPACITY
450    LET M3 = KG/1000
460    REM INCREASES VOLUME TO CORRECT FOR MOUTH AREA DEFORMATION
470    LET M3 = M3 * VCD:REM ALL FURTHER CALCS BASED ON THE NEW M3!
480    REM COMPUTES C FROM THE VOLUME
490    LET C = (V/M3)^(2/3)
500    LET SC = SQR(C)
510    REM COMPUTES SIGMA FROM C DELTARHO AND G
520    LET SIG = (998.71*9.800999)/C
530    REM RELATES SIGMA TO THE 42 LB/IN MAX OF MIL-SPEC NYLON
540    LET NYLSIG = (SIG*100)/7347.9
550    IF NYLSIG>=20 THEN K=1
560    REM COMPUTES YSIG BASED ON ELONGATION TESTS
570    REM EXPONENTIAL CURVE FIT FROM MACINTOSH CRICKET
580    YSIG = 11423*10^((2.4323E-04)*(SIG)):REM R^2 IS .96 FOR UP TO 2000 N/M
590    REM FIGURES A/V AT THE C ASSOCIATED WITH THE SELECTED CAPACITY
600    LET AV = (A/V)*SC
610    REM COMPUTES FORCE ON EACH HARNESS LEG
620    LET FH = (KG*10.81421)/N
```

```
630   IF FH >= 174 THEN K1 = 1
640   REM COMPUTES YH BASED ON ELONGATION TESTS
650   REM SIMPLE LINEAR REGRESSION FROM QUATTRO PRO
660   YH = 7.72*FH + 1078
670   REM FIGURES CIRCUMFERENCE
680   LET CIRC = 2*PI*XE/SC
690   REM SCREEN PRINTOUT OF INFO FOR USER EVALUATION
700   CLS
710   COLOR 15,1,0
720   PRINT "          PENDANT DROP UNDERWATER LIFT BAG DESIGN PROGRAM"
730   PRINT "MIL-C-7020G TYPE I MEMBRANE          MIL-C-5040 TYPE II HARNESS"
740   PRINT "              SHAPE FACTOR: LOG(B) = -0.24"
750   COLOR 15,2,0
760   PRINT "LIFT CAPACITY (KG)................................ ";KG
770   COLOR 15,1,0
780   PRINT "NUMBER OF GORES.................................. ";N
790   PRINT "FABRICATION TAKE-UP COMPENSATION COEFFICIENT..... ";FTU
800   PRINT "              CHARACTERISTICS AT FULL LOAD"
810   PRINT "VOLUME DISPLACED (M^3)............................ ";M3
820   PRINT "VOLUME CORRECTION COEFFICIENT.................... ";VCD
830   COLOR 15,2,0
840   IF K = 1 THEN COLOR 31,4,0
850   PRINT "MEMBRANE STRESS (SIGMA IN N/M)................... ";SIG
860   PRINT "        AS % OF U.T.S. OF MIL-C-7020G TYPE I...... ";NYLSIG
870   COLOR 15,1,0
880   PRINT "TENSILE MODULUS OF MEMBRANE (AT LOAD) (N/M)...... ";YSIG
890   PRINT "TOTAL SURFACE AREA (M^2)......................... ";A/C
900   PRINT "SURFACE TO VOLUME RATIO.......................... ";AV
910   PRINT "TOTAL HEIGHT, APEX TO HARNESS CONFLUENCE (CM).... ";100*SUMZ/SC
920   PRINT "ENVELOPE HEIGHT (CM)............................. ";100*Z/SC
930   PRINT "MOUTH DIAMETER (CM)............................. ";200*XM/SC
940   PRINT "MAXIMUM DIAMETER (CM)............................ ";200*XE/SC
950   PRINT "AXIAL DISTANCE ALONG GORE CENTERLINE (CM)........ ";S*100/SC
960   PRINT "MAXIMUM WIDTH OF A GORE (CM)..................... ";100*CIRC/N
970   PRINT "HARNESS LEG LENGTH (CM).......................... ";100*LH/SC
980   COLOR 15,2,0
990   IF K1 = 1 THEN COLOR 31,4,0
1000   PRINT "FORCE ON EACH HARNESS LEG (N).................... ";FH
1010   COLOR 15,1,0
1020   PRINT "TENSILE MODULUS OF HARNESS (AT LOAD) (N)......... ";YH
1030   INPUT "REDESIGN? (1=YES) ",Q1:IF Q1=1 THEN 100
1040   INPUT "HARDCOPY OF DESIGN AND CONSTRUCTION DATA? (1=YES) ",Q2
1050   IF Q2 <> 1 THEN 1730
1060   COLOR 31,4,0
1070   CLS:PRINT:PRINT:PRINT:PRINT:PRINT "WORKING........................"
1080   REM COMPUTES CORRECTION FACTOR FOR MEMBRANE DIMENSIONS
1090   LET CF = YSIG/(SIG+YSIG)
1100   REM COMPUTES CORRECTION FACTOR FOR HARNESS MATERIAL
1110   CFH = YH/(FH+YH)
1120   REM BEGINS HARDCOPY PRINTOUT
1130   LPRINT "          PENDANT DROP UNDERWATER LIFT BAG DESIGN PROGRAM"
1140   LPRINT "              SHAPE FACTOR: LOG(B) = -0.24"
1150   LPRINT "MEMBRANE: MIL-C-7020G TYPE I      HARNESS: MIL-C-5040 TYPE II"
1160   LPRINT "LIFT CAPACITY (KG)............................... ";KG
1170   LPRINT "BUOYANT FORCE (N)............................... ";KG*9.800999
1180   LPRINT "NUMBER OF GORES................................. ";N
1190   LPRINT "FABRICATION TAKE-UP CORRECTION COEFFICIENT....... ";FTU
1200   LPRINT "************CHARACTERISTICS AT FULL LOAD********************"
1210   LPRINT "VOLUME DISPLACED (M^3)........................... ";M3
1220   LPRINT "BUOYANT FORCE (N)............................... ";KG*9.800999
```

```
1230    LPRINT "MEMBRANE STRESS (SIGMA N/M)........................ ";SIG
1240    LPRINT "        AS % OF U.T.S. OF MIL-C-7020G TYPE I....... ";NYLSIG
1250    LPRINT "TENSILE MODULUS OF MEMBRANE (AT LOAD) (N/M)...... ";YSIG
1260    LPRINT "FORCE ON EACH HARNESS LEG (N)..................... ";FH
1270    LPRINT "TENSILE MODULUS OF HARNESS (AT LOAD) (N)......... ";YH
1280    LPRINT "C PARAMETER (M^-2)................................ ";C
1290    LPRINT "SQUARE ROOT OF C PARAMETER (M^-1).... ........... ";SQR(C)
1300    LPRINT "TOTAL SURFACE AREA (M^2).......................... ";A/C
1310    LPRINT "SURFACE TO VOLUME RATIO........................... ";AV
1320    LPRINT "TOTAL HEIGHT, APEX TO HARNESS CONFLUENCE (CM).... ";100*SUMZ/SC
1330    LPRINT "ENVELOPE HEIGHT (CM).............................. ";100*Z/SC
1340    LPRINT "MOUTH DIAMETER (CM)............................... ";200*XM/SC
1350    LPRINT "MAXIMUM DIAMETER (CM)............................. ";200*XE/SC
1360    LPRINT "AXIAL DISTANCE ALONG GORE CENTERLINE (CM)........ ";100*S/SC
1370    LPRINT "MAXIMUM WIDTH OF A GORE (CM)...................... ";100*CIRC/N
1380    LPRINT "HARNESS LEG LENGTH (CM)........................... ";100*LH/SC
1390    LPRINT "**********CONSTRUCTION DATA (IN CENTIMETERS)***************"
1400    LPRINT "     CORRECTED FOR STRESS AND FABRICATION TAKE-UP"
1410    LPRINT "AXIAL DISTANCE ON GORE     RADIAL DISTANCE FROM"
1420    LPRINT "CENTERLINE FROM APEX          GORE CENTERLINE"
1430    THD=5:S=.0502324:X=.0501687:GOSUB 1780
1440    THD=10:S=.10056:X=.10005:GOSUB 1780
1450    THD=15:S=.151079:X=.149356:GOSUB 1780
1460    THD=20:S=.201889:X=.197798:GOSUB 1780
1470    THD=25:S=.253091:X=.245086:GOSUB 1780
1480    THD=30:S=.304793:X=.29093:GOSUB 1780
1490    THD=35:S=.357109:X=.335036:GOSUB 1780
1500    THD=40:S=.410161:X=.377108:GOSUB 1780
1510    THD=45:S=.464083:X=.416846:GOSUB 1930
1520    THD=50:S=.519022:X=.453945:GOSUB 1780
1530    THD=55:S=.575144:X=.488092:GOSUB 1780
1540    THD=60:S=.632639:X=.518965:GOSUB 1780
1550    THD=65:S=.691726:X=.546228:GOSUB 1780
1560    THD=70:S=.752668:X=.569529:GOSUB 1780
1570    THD=75:S=.815783:X=.588486:GOSUB 1780
1580    THD=80:S=.881472:X=.602679:GOSUB 1780
1590    THD=85:S=.950257:X=.61163:GOSUB 1780
1600    THD=90:S=1.02285:X=.614764:GOSUB 1850
1610    THD=95:S=1.10029:X=.611348:GOSUB 1780
1620    THD=100:S=1.1842:X=.600344:GOSUB 1780
1630    THD=105:S=1.27748:X=.580079:GOSUB 1780
1640    THD=110:S=1.38647:X=.547169:GOSUB 1780
1650    THD=115:S=1.53332:X=.490549:GOSUB 2010
1660    LPRINT "HARNESS LEG LENGTH (M)....... ";(LH/SC)*CFH*100
1670    LPRINT
1680    LPRINT "DIMENSIONAL CORRECTION COEFFICIENT - MEMBRANE.... ";CF*FTU
1690    LPRINT "LENGTH CORRECTION COEFFICIENT - HARNESS.......... ";CFH
1700    LPRINT "VOLUME CORRECTION COEFFICIENT FOR DISTORTION..... ";VCD
1710    LPRINT "COMPLETE (PDULB24N.BAS)...................."
1720    LPRINT CHR$(12)
1730    COLOR 15,1,0
1740    CLS:PRINT:PRINT
1750    PRINT "PROGRAM TERMINATED........"
1760    FOR I = 1 TO 20:SOUND RND*1000+37,.4:NEXT I
1770    END
1780    LET DS = (FTU*S*CF*100)/SC:LET THR = THD*RAD
1790    THR=THD*RAD
1800    LET ARG = (SIN(PI/N)*SIN(THR))
1810    LET INVSIN = ATN(ARG/SQR(-ARG*ARG+1))
1820    LET ARC = (CF*FTU*100*X*INVSIN)/(SIN(THR)*SC)
```

44

```
1830   LPRINT USING "     ###.####                    ###.####";   DS,ARC
1840   RETURN
1850   REM FOR EQUATOR
1860   LET DS = (FTU*S*CF*100)/SC:LET THR = THD*RAD
1870   LET THR=THD*RAD
1880   LET ARG = (SIN(PI/N)*SIN(THR))
1890   LET INVSIN = ATN(ARG/SQR(-ARG*ARG+1))
1900   LET ARC = (CF*FTU*100*X*INVSIN)/(SIN(THR)*SC)
1910   LPRINT USING "     ###.####              ###.#### (THD=90)";   DS,ARC
1920   RETURN
1930   REM THETA = 45
1940   LET DS = (FTU*S*CF*100)/SC:LET THR = THD*RAD
1950   LET THR=THD*RAD
1960   LET ARG = (SIN(PI/N)*SIN(THR))
1970   LET INVSIN = ATN(ARG/SQR(-ARG*ARG+1))
1980   LET ARC = (CF*FTU*100*X*INVSIN)/(SIN(THR)*SC)
1990   LPRINT USING "    ###.####              ###.#### (THD=45)";   DS,ARC
2000   RETURN
2010   REM THETA AT 115 (TRUNCATION)
2020   LET DS = (FTU*S*CF*100)/SC:LET THR = THD*RAD
2030   LET THR=THD*RAD
2040   LET ARG = (SIN(PI/N)*SIN(THR))
2050   LET INVSIN = ATN(ARG/SQR(-ARG*ARG+1))
2060   LET ARC = (CF*FTU*100*X*INVSIN)/(SIN(THR)*SC)
2070   LPRINT USING "    ###.####              ###.#### (THD=115)";   DS,ARC
2080   RETURN
```

REPORT DOCUMENTATION PAGE

Public reporting burden for this collection of information is estimated to average 1 hour per response, including the time for reviewing instructions, searching existing data sources, gathering and maintaining the data needed, and completing and reviewing the collection of information. Send comments regarding this burden estimate or any other aspect of this collection of information, including suggestions for reducing this burden, to Washington Headquarters Services, Directorate for Information Operations and Reports, 1215 Jefferson Davis Highway, Suite 1204, Arlington, VA 22202-4302, and to the Office of Management and Budget, Paperwork Reduction Project (0704-0188), Washington, DC 20503.

1. AGENCY USE ONLY *(Leave blank)*	2. REPORT DATE March 1993	3. REPORT TYPE AND DATES COVERED Contractor Report

4. TITLE AND SUBTITLE

Advanced Underwater Lift Device

5. FUNDING NUMBERS

6. AUTHOR(S)

David T. Flanagan
* Robert C. Hopkins

7. PERFORMING ORGANIZATION NAME(S) AND ADDRESS(ES)
Krug Life Sciences
Houston, TX 77058

* University of Houston, Clear Lake
Houston, TX 77058

8. PERFORMING ORGANIZATION REPORT NUMBER

9. SPONSORING / MONITORING AGENCY NAME(S) AND ADDRESS(ES)

NASA
Johnson Space Center
Houston, TX 77058

10. SPONSORING / MONITORING AGENCY REPORT NUMBER

CR 185709

11. SUPPLEMENTARY NOTES

12a. DISTRIBUTION / AVAILABILITY STATEMENT

Unclassified/Unlimited
Subject Category 14

12b. DISTRIBUTION CODE

Unlimited

13. ABSTRACT *(Maximum 200 words)*

Flexible underwater lift devices ("lift bags") are used in underwater operations to provide buoyancy to submerged objects. Commercially available designs are heavy, bulky, and awkward to handle, and thus are limited in size and useful lifting capacity. An underwater lift device having less than 20% of the bulk and less than 10% of the weight of commercially available models has been developed. The design features a dual membrane envelope, a nearly homogeneous envelope membrane stress distribution, and a minimum surface-to-volume ratio. A proof-of-concept model of 50 kg capacity was built and tested. Originally designed to provide buoyancy to mock-ups submerged in NASA's weightlessness simulators, the device may have application to water-landed spacecraft which must deploy flotation upon impact, and where launch weight and volume penalties are significant. The device may also be useful for the automated recovery of ocean floor probes or in marine salvage applications.

14. SUBJECT TERMS

marine technology, underwater structures, lift devices, spacecraft recovery, flotation

15. NUMBER OF PAGES
49

16. PRICE CODE

17. SECURITY CLASSIFICATION OF REPORT Unclassified	18. SECURITY CLASSIFICATION OF THIS PAGE Unclassified	19. SECURITY CLASSIFICATION OF ABSTRACT Unclassified	20. LIMITATION OF ABSTRACT Unlimited

NASA-JSC